Response to Anonymous Referee #1

Thank you very much for your constructive and careful comments. It was greatly helpful to improve the quality of the draft.

****Note) Following the request of Anonymous Referee #3, Figure 1 was divided into Figure 1 and 2. So, the figure numbers of subsequent figures were increased by 1.**

Major Comments:

1 . Sizes of figures and characters in figures

Sizes of figures and characters in figures are too small to see. Figures 2, 3 and 4 should be much larger. I recommend the authors to move panels of z_{LCL}, z_{inv}, α, and $1-\beta_2$ in these figures to supplement, and to divide Figs. 2 and 3 further in order to make the panels larger. Sizes of characters in Fig. 6, 7 should be larger. It is also desirable that sizes of tic marks of color bars in Fig. 1 and sizes of characters in Fig. 8 are larger.

➔ Thank you for the suggestion. Following the comment, we divided Figures 3, 4, and 5. In addition, the panels of z_{LCL}, z_{inv}, α, and $1-\beta_2$ are moved to supplement (S1, S2, S3). The size of the characters in Fig. 7, 8 is enlarged, and the sizes of tic marks of color bars in Fig. 2 and the sizes of characters in Fig. 9 are enlarged too.

2 . Labels for cloud types

Cloud types are labeled as CL11, CL6, CL5, … I understand that they are labels based directly on the WMO classification and they have some advantages. However, it is very complicated when we read the manuscript because readers cannot easily remember the labels. Could you relabel them as, for instance, Fog, St, Sc, … or FOG, ST, SC, …, or CL_Fog, CL_St, CL_St, …?

➔ Following the comment, we relabeled all the cloud types, and Table 2 is added to explain the abbreviations. Please see P5L10-13 in the tracked-change version.

3 . Short physical explanations are needed in many parts

In many parts in the text, physical explanations that attribute the results to the characteristics of proxies are not enough. I guess they are helpful for readers even if they are just one or a few sentences. For example:

P6L22-23:

"both LTS and EIS increase, particularly over the far northern continents and Arctic area."

Please provide a suggestion of the reason why LTS and EIS increase in the situation.

➔ This is because noCL (no low-level cloud) can occur when inversion is strong near the surface under dry conditions. We added the explanation in P7L10-12.

P6L32-33:

"undesirable negative anomalies of LTS and EIS over the far northern continents including Arctic area get worse from CL11 to CL6 and CL7"

Please provide an interpretation of the reason why LTS and EIS show negative anomalies.

➔ We speculate that in these dry regions, the formation of Fog (CL11), F.St (CL6), and B.St (CL7) needs upward moisture transports from the surface, which is likely to be accompanied by the reduction of vertical stability in the lower troposphere. We added the explanation in P7L25-28.

P7L5-7: "over the Arctic, Asia, and deserts areas, LTS/EIS shows negative anomalies opposite to the increased LCA, which worsens and extends to other continents from CL5, CL84 to CL12 and CL39"

Please provide a suggestion of the reason why LTS/EIS shows negative anomalies over the areas.

➔ The negative correlation for Sc (CL5) can be explained by the same physical processes applied to the cases of Fog, F.St, and B.St as explained above. In the very dry regions where background LCA is very small, the onset of Cu (CL12) and Cb (CL39) in the low LTS/EIS

situations will result in the increase of LCA. We added the explanation in P8L3-6.

P7L22: "LTS and EIS, which have strong ocean-land contrasts (in particular, EIS) and seasonal cycle over land."

Please explain why ELF does not have strong ocean-land contrasts and seasonal cycle over land but LTS and EIS have them.

➔ The weaker seasonal cycle and ocean-land contrasts of ELF may imply the opposite variations in z_{inv} and z_{LCL}. The freezedry factor also contributes to reducing the excessive seasonal cycle. We added the explanation in P8L21-22 and P8L23.

P7L24: "with a larger ELF during the night"

Please explain why ELF is larger during the night.

➔ This is presumably due in part to diagnosing of noCL condition as a non-zero ELF. We added the explanation in P8L24-25.

P7L34: "with systematically higher proxy values"

Can you guess why night slopes have systematically higher proxy values?

➔ It indicates that the product of z_{inv} and z_{LCL} during the day is larger than that during the night. We added the explanation in P9L1-5.

P7L34-35:

"both ELF and 1-β2 tend to have steeper regression slopes during the night than during the day"

Can you guess why regression slopes are steeper during the night than during the day?

➔ This is due in part to the diagnosis of noCL condition as a non-zero ELF, particularly, during

the night when noCL conditions are frequently reported. We added the explanation in P9L6-7.

Fig. 5c: The CL0 plots in Fig. 5c are against our simple tuition from previous studies (e.g., Wood and Bretherton (2006), Kawai et al. (2017)). This may confuse readers. Please briefly explain the reason of the apparent difference between CL0 plots in Fig. 5c and conventional figures.

➔ In responding to your comments above and below, we included explanations on this in P7L11-12 and P9L29-32 of the tracked-change version.

P8L15: "The frequency of CL0 increases as LTS and EIS increase"

This is against our simple intuition, at least, over the ocean. What causes this increase over the ocean? Mainly where? In what season and what situation?

➔ We note that noCL condition is frequently reported with a strong inversion at near the surface when LTS/EIS is large. We added the explanation in P9L29-32.

P8L32: "The freezedry factor substantially contributes to the improved correlations of CL0 with ELF from β2"

Please briefly explain the physical meaning (for example, where and in what situation the factor mainly contributes to the improvement of the correlations).

➔ As explained in PS19, the freezedry factor is designed to reduce a diagnosed LCA in a very dry region, such that it is most effective over the far northern continents and Arctic area, particularly during winter. We added the explanation in P10L16-18.

P8L33-34:

"the frequent occurrence of CL0 on the west coast of the major continents and equatorial SST cold regions"

I guess that people do not expect that the occurrence of CL0 is frequent on the west coast of

the major continents. Please add a little more explanation or note.

➔ The frequent occurrence of noCL on the west coast is due to the advection of dry air from nearby continents. The frequent occurrence of noCL over the SST cold tongue is due to the warm air advection from the south. We added the explanation in P10L20-23

4 . Target areas of LTS, EIS, and ECTEI

Please emphasize repeatedly in the text for fairness that the target areas of LTS, EIS, and ECTEI are over the ocean without sea ice and it is not intended to be used over land and sea ice.

➔ Following your comment, we emphasized repeatedly that the target area of LTS/EIS/ECTEI are over the ocean. Please see P7L29-30 and P11L16-17 in the tracked-change version.

5 . Comparison of EIS and LTS

It is well-known that EIS is an index much better than LTS over the ocean. However, it is not so clear in the author's study. I guess readers will be confused. Please discuss a little why the superiority of EIS to LTS over the ocean is not clear in this study.

➔ It is well known that EIS is better than LTS in the marine stratocumulus deck regime. However, our analysis domain is not confined in the marine stratocumulus deck but extended into the entire globe with various cloud regimes. Because of this, it seems that the superiority of EIS over LTS is not clearly seen in our analysis. We briefly explained this in a revised draft in P9L11-14.

6 . Discuss pros and cons of ELF compared with LTS/EIS/ECTEI.

Pros are very clear, I guess. Cons of ELF could be, for example:

*** LTS/EIS/ECTEI tend to represent optically thick stratocumulus. It is important for earth radiation budget. Can ELF be directly used for discussions related to radiation budget?**

*** LTS/EIS/ECTEI are based on very simple concept. ELF and the proposed idea for improvement of ELF seem to be very empirical.**

(* Discussion utilizing ELF or improved ELF could be complicated to understand LCA or LCA

changes.)

(* LTS/EIS/ECTEI are very simple and easily calculated.)

① LTS/EIS/ECTEI tend to represent optically thick stratocumulus. It is important for earth radiation budget. Can ELF be directly used for discussions related to radiation budget?

➔ ELF is designed to predict LCA of all types of clouds, so it can be used globally to discuss the radiation budget.

② LTS/EIS/ECTEI are based on very simple concept. ELF and the proposed idea for improvement of ELF seem to be very empirical.

➔ While the computation of ELF or improved ELF seems more complicated than LTS/EIS/ECTEI, we think that it is not so complicated. EIS needs θ_{sfc}, θ_{700}, z_{LCL} and moist adiabatic lapse rates at z_{LCL} and z_{700} (Γ_{LCL} and Γ_{700}) to calculate, and these are all information needed to calculate ELF too (if freezedry factor is ignored).

③ Discussion utilizing ELF or improved ELF could be complicated to understand LCA or LCA changes

➔ ELF (or improved ELF) can be useful to understand LCA changes. Please refer to the response to the comment below.

➔ It seems like the apparent con of ELF is that its formulation is bit complicated and empirical. We briefly discuss of pros and cons of ELF at P15L9-12 in the tracked-change version.

7. Section 3.5

I'm afraid that proposed idea for improvement of ELF is too much empirical and complicated, although I understand the value of the challenge. Is it needed to construct a unified proxy for LCA by making a tremendous effort, even though the cloud regimes and mechanisms that produce LCA are quite different? Please discuss it a little.

➔ The reason why we need a more precise unified proxy may be explained in relation to the cloud feedback. As shown in our paper, the response of LCA to environment variables is non-linear and varies depending on cloud types. Thus, to investigate the climate sensitivity of low-level clouds globally, it may be good to use a unified proxy, such as ELF. The contribution of individual environment variables can be extracted by linearizing ELF

formulation (e.g. $\Delta \mathrm{ELF} \approx \frac{\partial \mathrm{ELF}}{\partial z_{\mathrm{inv}}} \Delta z_{inv} + \frac{\partial \mathrm{ELF}}{\partial z_{\mathrm{LCL}}} \Delta z_{LCL} + \frac{\partial \mathrm{ELF}}{\partial \mathrm{f}} \Delta f$). In this way, we can describe the physical processes controlling low cloud feedback, which depends on cloud regimes, in a single framework. As noted by the reviewer, the development of an advanced ELF may take lots of time and effort. However, due to the reasons mentioned above, we think it is worthwhile to do that. We briefly included this discussion in P15L9-12.

8 . Short discussion on cloud feedback

In the first paragraph of the introduction, the manuscript mentions an importance of the impact of low-level clouds on the Earth's climate including cloud feedback and climate sensitivity. However, there are no descriptions or suggestions on cloud feedback later in the manuscript, although this is a critically important topic now. Although the manuscript does not discuss it at all, proxies LTS, EIS, and ECTEI cause quite different estimation of cloud feedback. LTS causes strong negative cloud feedback, EIS suggests weak negative feedback, and ECTEI suggests positive cloud feedback over the ocean (models and observations imply positive cloud feedback, that is, a decrease in low-cloud in warmer climates). Could the authors add a short discussion or comments on cloud-feedback based on ELF?

➔ Thank you very much for the very nice comments. As noted by the reviewer, exploring cloud feedback and climate sensitivity is an extremely important subject. Following the comments, we examined the climate sensitivity diagnosed by ECTEI, LCA, and ELF. The below figure shows the SST dependency of ECTEI, LCA, and ELF over the ocean. ECTEI is one of the unified LCA proxies which accounts SST dependency of LCA by including cloud top entrainment criteria. As shown in the figure, ECTEI is tightly dependent on SST and EIS, but the scatters of LCA and ELF are more divergent. This implies that cloud controlling factors other than SST and EIS should work for the observed LCA. Both ECTEI and ELF predict the negative LCA slope to SST for a fixed EIS, which is known to compensate the LCA increase in a warm climate in association with higher EIS. The ELF-predicted SST slope is -0.66 % K^{-1}, which is smaller than that of LCA (-1.66) and ECTEI (-0.80). This result indicates a need to develop a more advanced ELF.

➔ As noted by the reviewer, exploring climate sensitivity is extremely important and a huge research subject. However, a detailed examination of climate sensitivity seems to be out of the main theme of our current draft, which focused on the relationship between LCA and various proxies by cloud types.

➔ So, we think that it will be better to explore climate sensitivity in a separate paper in a more comprehensive way, which, in fact, is one of our future research subjects. Following the comments, this future research plan is briefly explained in the conclusion section (P15L15-

17).

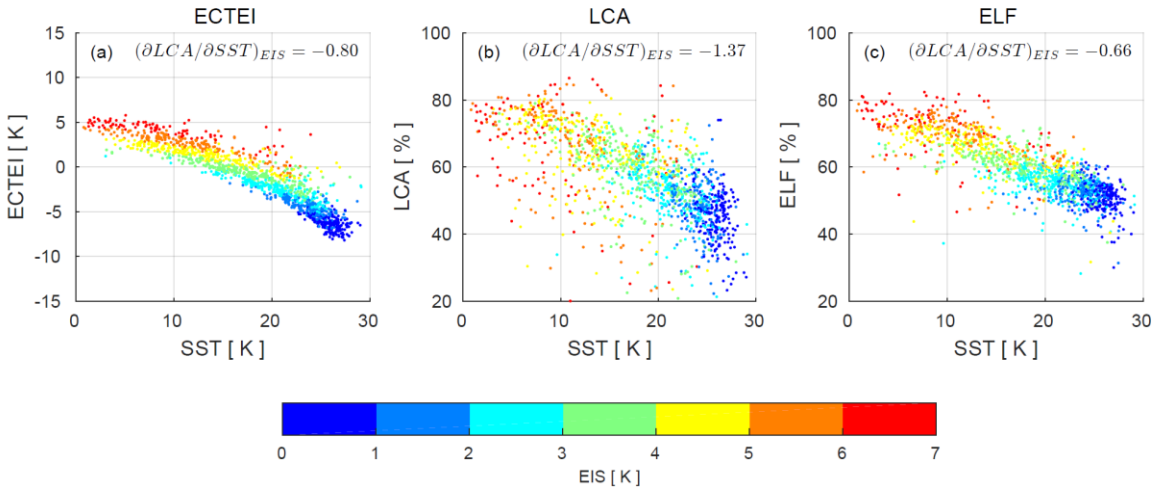

Figure 1. Scatter diagrams showing SST dependency of ECTEI, LCA, and ELF for each EIS bin (denoted by different colors). All seasonal climatologies of 5° latitude x 10° longitude ocean grids boxes between 60°N and 60°S are used in the analysis. The mean SST slope ($[\partial LCA/\partial SST]_{EIS}$ in units of $[\,\%\,K^{-1}]$) denoted at the top of each panel is calculated by doing a linear regression for each EIS bin and averaging the regression coefficients of all EIS bin. For ECTEI, a conversion factor between LCA and ECTEI is assumed as dLCA/dECTEI = 3.1 $\%\,K^{-1}$ following Kawai et al. (2017).

Minor comments:

Somewhere:

Is a variable β2 defined somewhere?

➔ We added the definition of β2 in P3L21-23.

P1L8-9: "the decrease in LCA when CL0 is reported and the increase of LCA when CL12 is reported"

Are "decrease" and "increase" appropriate? It is not easy to understand, especially if readers don't read the contents yet, I guess.

➔ Following the comment, we removed the wording of "increase" and "decrease", and changed

them to "changes". Please see P1L8-9 in the tracked-change version.

P1L13: "the dissipation of LCA"

Is the word "dissipation" appropriate?

➔ The phrase "dissipation of" has been modified to "decrease of" for clarity. Please see P1L13 in the tracked-change version.

P7L31: "a high EIS located outside of the plotting range" Can't you widen the range of the figure?

➔ Following the comment, we have widened the range of the figure. Following the comment of referee #2, the squared regression coefficients (R^2) without Fog are added in Figure 6. Thus, we rewrote the sentence. Please see Figure 6 and P8L31-34 in the tracked-change version.

P8L5: "Figure 6 is the cumulative plot"

Caption in Fig.6: "Cumulative FQ"

Is Fig. 6 a cumulative plot? I though this is just a percentage plot.

➔ The more appropriate name of the plot is "stacked percentage plot". Please see the caption of Figure7 and P9L16 in the tracked-change version.

Caption of Fig. 5:

Explain the difference between open and filled symbols.

➔ Thank you for pointing out. We added the explanation in the caption of Figure 6.

Fig. 6c, 6e:

Why do LTS (and also EIS) have a large difference between daytime and night time over the ocean? It is understandable that there is a large difference over land (LTS and EIS is smaller in daytime). But why over the ocean also? I thought diurnal variations of LTS and EIS is negligible over the ocean because the SST diurnal variation is very small.

➔ It seems that the reviewer mis-interpreted Fig.7c and 7e. As was explained in the caption of Fig.7, "The bright and dark colors in each bar denote the fractions during the daytime and nighttime, respectively", instead of representing the values of LTS (or EIS) during the daytime and nighttime.

Fig.6e: Please briefly explain the reason why the black line is very insensitive to EIS over the ocean. I guess many readers will be embarrassed because they often see the very clear relationship between LCA and EIS over the ocean in several papers (e.g., Wood and Bretherton (2006), Kawai et al. (2017)). Please clarify the cause of the differences.

➔ As explained before, the high correlation between EIS and LCA reported in previous studies is mainly for the case of stratocumulus (CL5, CL6, CL84). In our study, however, we are examining the correlation across the entire low cloud types, such that the correlation between EIS and LCA is not large, as shown in Fig.6. This explanation is added in P9L32-34.

Caption of Fig. 6:

100 -> 100 %

➔ Corrected. Please see the caption of Figure 7.

Response to Anonymous Referee #3

Thank you very much for your constructive and careful comments. It was greatly helpful to improve the quality of the draft.

****Note) Following the request of Anonymous Referee #3, Figure 1 was divided into Figure 1 and 2. So, the figure numbers of subsequent figures were increased by 1.**

Major issues

1. Jargon

The almost exclusive use of cloud type numbers (e.g., CL12) makes this paper extremely difficult to follow. (As a side note, "CL" is not a terribly intuitive abbreviation of cloud type either.) Table 1 is helpful but not sufficient, and does not list the combined types defined by the authors.

The authors should standardize how they describe each major cloud classification used (e.g., CL12 could be "shallow-to-moderate cumulus") and try to pair the descriptive words with the cloud type number as often as possible. Page 8, Line 29 does this very well — something like this should be done for the entire paper (including figure captions).

➔ Following the comment, we relabeled all the cloud types, as explained in Table 2. Please see P5L10-12 in the tracked-change version.

2. Treatment of LTS, EIS, and ECTEI

I am confused by the authors' treatment of LTS and EIS as low cloud "proxies" rather than as cloud-controlling factors. Clearly LTS and EIS correlate with stratiform clouds, but the strength of the boundary layer inversion is really only one relevant factor among several in explaining low cloud behavior. LTS/EIS can certainly be used as proxies for low cloud fraction, but this is not their primary/sole purpose.

Similarly, LTS/EIS really don't "diagnose" anything (e.g., Page 8, Lines 19-20). They are cloud-controlling factors (one of many!), not simple diagnostics in and of themselves.

This conceptual treatment leads to several statements that sound off, at least to my ears. For instance, on Page 9, Lines 4-5, is it truly "undesirable" that we can associate particularly large values of LTS/EIS with cloud clearing? This could be a useful observation to better understand

potentially non-linear cloud behavior. This seems to me like a strange way to conceptualize LTS/EIS and why one would examine these variables.

The authors mention ECTEI in the abstract and (barely) define it in the introduction before noting it is similar to EIS and therefore not shown at the end of the Methods section. I would recommend having a supplement with the ECTEI results or not mentioning it at all (or only as a parenthetical). As written, the authors appear to promise an analysis they do not deliver.

➔ We used the term "proxy" for the LTS and EIS, in order to keep consistency with our previous paper (Park and Shin 2019; PS19) which already used LTS and EIS as one of LCA proxies. At least in stratiform cloud regions, LTS and EIS have been used as proxies of LCA in many papers. Many readers will be familiar with this and there won't be much difficulty in understanding the concept. However, we agree that several statements could confuse some readers. Thus, following the comment, we modified the following.

①**"Clearly LTS and EIS correlate with stratiform clouds, but the strength of the boundary layer inversion is really only one relevant factor among several in explaining low cloud behavior."**

➔ We agree with the comment and included this explanation in P2L14-15.

② **"Similarly, LTS/EIS really don't "diagnose" anything (e.g., Page 8, Lines 19-20). They are cloud-controlling factors (one of many!), not simple diagnostics in and of themselves."**

➔ Following the comment, we rephrased this sentence. Please see P10L1-3.

③ **"on Page 9, Lines 4-5, is it truly "undesirable" that we can associate particularly large values of LTS/EIS with cloud clearing? This could be a useful observation to better understand potentially non-linear cloud behavior. This seems to me like a strange way to conceptualize LTS/EIS and why one would examine these variables. "**

➔ We agree that the word "undesirable" is not appropriate here. Thus, we changed the word "undesirable" to "unexpected".

➔ We also noted that the strong positive correlation between LTS/EIS and noCL FQ might indicate a non-linear response of clouds to the inversion strength or the existence of other factors controlling noCL. Please see P10L27-30 in the tracked change version.

➔ In addition, we stated that the target areas of LTS, EIS, and ECTEI are over the ocean. Please see P7L29-30 and P11L16-17 in the tracked-change version.

③ The authors mention ECTEI in the abstract and (barely) define it in the introduction before noting it is similar to EIS and therefore not shown at the end of the Methods section. I would recommend having a supplement with the ECTEI results or not mentioning it at all (or only as a parenthetical). As written, the authors appear to promise an analysis they do not deliver.

➔ Following the comment, we removed ECTEI from the abstract. Although not shown, the analysis results of ECTEI are **almost identical** to EIS as mentioned at the end of the Methods section (P5L25). Thus, we did not include the results of ECTEI in the supplement.

3. Definition of "low-level" cloud and its reasonableness

While the observer-based methods define deep convection as "low-level" cloud based on the cloud base, there should be some discussion/reflection of whether this is a reasonable treatment in this analysis. LTS/EIS really are meant to explain cloud behavior in shallow boundary layers, not in deep convection. I don't particularly understand why we should expect one equation or metric to apply globally for both shallow and deep convection. If the authors do have a good explanation for this, it would be very helpful to provide it.

➔ Because deep convection is controlled by similar physical processes as shallow convection (Park 2014a,b), it is unnecessary to use separate formulation for shallow and deep convections. In addition, at least in terms of cloud fraction, we thought that a decoupling hypothesis can describe the changes in cloud fraction from the well mixed (Sc), partially decoupled (Sc-Cu), and fully decoupled (Cu, Cb) conditions. This is the philosophy of ELF. We briefly included this explanation in P5L13-14.

4. Missing variable in the derivation of ELF

Many times in the manuscript, the authors refer to and analyze a factor (1 - β2), but this is never defined. Please address this in the methods section. It also might be possible to reorganize the section deriving ELF to be more clear, especially with an eye toward the issues brought up in the final discussion of possible improvements for an "advanced ELF." Although the finer details of the ELF calculation addressed previously do not need to be explained in great detail, it should not be expected that all readers are familiar with PS19.

➔ Following the comment, the definition of (1 - β2) is added in P3L22-23 in the tracked-change version. We also reorganized the structure of explaining the definition of ELF (P3L21-P4L6). We did not add very detailed derivation of ELF here, because it requires a lengthy explanation of the conceptual framework with a diagram.

5. General presentation and organization of figures

The figures are far too crowded, and each subpanel much too small, to be easily interpreted by readers. In Figures 1-3, the black contours showing the climatology are nearly illegible. For Figure 1, a suggestion could be to split the figure up by cloud type (as is done for Figures 2-3) and have an added column for the climatology in its own map.

➔ Following the comment, we divided Figure 1 to Figure 1 and Figure 2.

For Figures 2-3, I would also recommend subdividing further. One solution could be to have one figure include ELF and comparisons to LTS/EIS in one figure and the components of ELF in another. This could also help structure the discussion — first the differences between ELF, LTS, and EIS can be discussed, and then the contributions of the different components of ELF can be discussed.
It may also be a good idea to split up Figure 4 in a similar manner.

➔ Following the comment, we divided Figures 3, 4, and 5 (previously Figures 2-4) and panels of z_{LCL}, z_{inv}, α, and 1-β_2 are moved to supplement (S1, S2, S3).

In Figure 5, the caption should explain that the color scheme is the same as that used in Figure 4. The open versus closed symbols also are not defined, although I assume they relate to day and night.
For the regressions in Figure 5, it would be good to address to what extent CL11 drives the regressions. Especially for subpanels b) and d), the scatter of points excluding CL11 (and CL0 and CLIM) do not appear to be very strongly correlated.

➔ In the caption of Figure 6, we explained that the color scheme used is the same as that used in Figure 5. The open and closed symbols are explained too.
➔ Following the comment, we also added squared regression coefficients (R^2) without Fog (CL11) in parenthesis. A corresponding explanation is written in P8L31-34 in the tracked-change version.

In Figure 8, the caption should make more clear that the adjustable scale height as a function of the environmental variables in g) and h) is shown as the "viridis" shading and is in units of meters.

➔ In the caption of figure 9, we specified that the adjustable scale height is shown as shading and in units of meters.

6. Interpretation of ELF correlation with cumulus cloud fraction in Tables 2 and 3

On Page 12, Line 12, the authors write that ELF captures variations in cumulus clouds (CL12) better than LTS and EIS. Unless there is a typo in the tables, this is contradicted by the evidence provided in Tables 2 and 3. The global correlation of ELF with CL12 is ~0.03 whereas it is between -0.45 and -0.75 for LTS and EIS. Or is this sentence actually referring to CL84? In that case, the correlations are more all over the map. In any event, this is another good example of where the elimination of jargon in favor of clearly indicating which cloud type is being discussed would be helpful.

➔ It seems that the reviewer misunderstood. Tables 3 and 4 do not show the correlations between proxies and LCA; they show the correlations between proxies and **the frequency (FQ)** of individual cloud type. If any proxy is perfect, the correlation between the perfect proxy and CL FQ should be identical to the correlation between the LCA and CL FQ.

➔ As an example: The global correlation between cumuli's LCA and FQ is 0.10. ELF has a similar correlation of -0.03. LTS and EIS have the correlation values of -0.45 and -0.75. In this case, ELF is a better proxy for LCA than LTS and EIS.

Specific issues

Page 1, Line 18: As the citation of Klein & Hartmann (1993) suggests, the efforts to quantify low cloud effects on Earth's climate long predate the last decade.

➔ We changed "last decade" to "past few decades". Please see P1L17 in the tracked-change version.

Page 2, Line 14: If you do choose to include ECTEI, its definition needs more exposition here.

➔ Following the comment, we added the definition of ECTEI in the Method section. Please see lines P3L17-20 in the tracked-change version.

Page 3, Eq. (5): It would be helpful to discuss that you then force the inversion height to lie between the LCL and the LCL plus a scale height in your analysis here. It's easy to miss as written. Also, for shallow convection, there's essentially no way for the inversion height to exceed the LCL plus scale height, right?

➔ Following the comment, the range of the inversion height is added in Eq. (6). Please see P3L25 in the tracked-change version. As you said, the inversion height cannot exceed LCL plus scale height, but since scale height is Δz_s = 2750m, the upper limit of inversion height can easily exceed the height of 700hPa.

Page 4, Line 9: "f" does not denote the amount of water vapor, it is a function of water vapor.

➔ We specified that "f" is an increasing function of water vapor. Please see P4L14 in the tracked-change version.

Page 4, Line 25: Individual components of ELF really aren't "proxies" for low cloud fraction by themselves. It would be more straightforward to just discuss these as components of ELF.

➔ We rewrote the sentence. Please see P5L1-3 in the tracked-change version.

Page 4, Line 32: It would be helpful to explain that cloud types 12, 84, and 39 are actually combinations of types 1+2, 8+4, and 3+9.

➔ The combination of the cloud types are explained in Table2. Please see P5L10-13 in the tracked-change version.

Page 5, Lines 15-16: Moisture supply is not the only difference between marine and continental boundary layers (different responses to diurnal solar heating comes to mind as potentially being important here too).

➔ We specified that the moisture supply is "one of the important factors", rather than "primary factor". Please see P5L29-30 in the tracked-change version.

Page 5, Line 25: I would expect the relative humidity to matter more than the total amount of moisture here, no?

➔ In the far northern continents and Arctic area, the freezedry factor, which is a function of the absolute moisture amount, becomes very important for the onset of noCL. The relative humidity is also important but the amount of moisture is a more comprehensive concept.

Page 5, Lines 28-29: It would be helpful here to discuss how much of the advantage ELF has over LTS/EIS/ECTEI is due to the freezedry factor alone.

➔ First, we briefly explained why ELF is improved by the freezedry factor in P6L11-12. The quantitative improvements are already investigated in our previous study, so we cited the paper (PS19) here.

➔ The effect of the freezedry factor is discussed many times in subsequent sections (e.g. P7L13, P8L23).

Page 6, Lines 5-7: Why isn't the composite analysis shown? It could at least be included in a supplement. The result isn't particularly surprising but would be interesting to see.

➔ The composite is not shown here because it will be included in the paper we are preparing. We cited the paper so future readers could find corresponding figures. Please see P6L23 in the tracked-change version.

Page 6, Line 10: Why is there no hemispheric asymmetry in stratocumulus amount? If meteorology is the main driver, one would expect the hemispheric trends to be out of phase. In the Southern Hemisphere, the seasonal cycle tends to peak in spring and trough in fall whereas the Northern Hemisphere tends to peak in summer and trough in winter, so perhaps only looking at JJA-DJF differences doesn't capture the Southern Hemisphere seasonality well. Discussing SON and MAM seasonality (even if not shown, or just put in supplement) could be useful here.

➔ As Klein and Hartmann (1993) shown, stratiform clouds in the Namibian and Peruvian stratocumulus decks tend to peak in SON. Since the detailed analysis on the seasonal cycle is not the scope of our paper, we just cited Klein and Hartmann (1993) here. Please see P6L28-30 in the tracked change version.

Page 6, Line 20: It would be helpful to explain why the non-centered correlation is computed in some sections a centered correlation is computed in others, and whether this has any implication for the interpretation of your results.

➔ We explained why the non-centered correlation is computed here. Please see P7L7-9 in the tracked change version.

Page 7, Lines 25-27: The latent cooling effect of evaporation should also matter for lowering the LCL.

➔ Corrected. Please see P8L28 in the tracked-change version.

Page 7, Line 31: Please either indicate what the outlier value is on the plot or report it here.

➔ We extended the range of x-axis of Figure 6, so the scatter located outside of the plot is now located inside of the plot. Please see Figure 6, and also see P8L31-34 in the tracked-change version.

Page 8, Section 3.3: It would be helpful somewhere here to explain clearly what the difference between LCA and AMT is and how this should be interpreted.

➔ Following the comment, we added an explanation of the difference between LCA and AMT in Section 3.4. Please see P10L32-33 in the tracked-change version.

Page 9, Line 28: "What is necessary" should replace "What are necessary".

➔ Corrected. Please see P11L20 in the tracked-change version.

Page 12, Line 24: What does the "(stratiform clouds FQ)" mean here in context? Is it supposed to refer to an increase in stratiform clouds as cumuliform cloud FQ decreases?

➔ "Increase in" is mistakenly omitted here, so we corrected it. Please see P14L19 in the tracked-change version.

Page 13, Line 6: What would a negative depth for the decoupled layer mean physically? Wouldn't it just make more sense to define ELF piecewise rather than as a continuous function to account for these types of circumstances?

- ➔ Following the comment, we explained the physical meaning of a negative decoupled layer depth at P12L1-2 in the tracked-change version.
- ➔ As you commented, it can be one option to define ELF piecewise by separating the cases where a decoupled layer has negative depth or positive depth. However, such a strategy does not seem to work well when we tested it. Probably because the calculation of the inversion height is not accurate.

Page 13, Line 12: I do not understand what the "if any" means here. Surely you believe there is some appropriate variable, or why even discuss parameterizations of the scale height?

- ➔ It seems like "if any" is unnecessary here, so it is deleted. Please see P15L7 in the tracked-change version.

Page 13, Line 18: It would be good to list the download site for the ERA data here as well.

- ➔ Following the comment, we listed the download site for the ERA data. Please see P15L18-19 in the tracked-change version.

The Relationship between Low-Level Cloud Amount and Its Proxies over the Globe by Cloud Types

Jihoon Shin and Sungsu Park

School of Earth and Environmental Sciences, Seoul National University, Seoul, South Korea

Correspondence: Sungsu Park (sungsup@snu.ac.kr)

Abstract. We extend upon previous work to examine the relationship between low-level cloud amount (LCA) and various proxies for LCA - estimated low-level cloud fraction (ELF), lower-tropospheric stability (LTS), and estimated inversion strength (EIS) ~~, and estimated cloud-top entrainment index (ECTEI)~~ - by low-level cloud types (CL) over the globe using individual surface and upper-air observations. Individual CL has its own distinct environmental structure, and therefore our extended analysis by CL can provide insights into the strength and weakness of various proxies and help to improve them.

Overall, ELF performs better than LTS/EIS in diagnosing the variations in LCA among various CLs, indicating that a previously identified superior performance of ELF to LTS/EIS as a global proxy for LCA comes from its realistic correlations with various CLs rather than with a specific CL. However, ELF as well as LTS/EIS has a problem in diagnosing the ~~decrease~~ changes in LCA when ~~CL0~~ noCL (no low-level cloud) is reported and ~~the increase of LCA when CL12~~ also when Cu (cumulus) is reported over the deserts where background stratus does not exist. This incorrect diagnosis of ~~CL0~~ noCL as a cloudy condition is more clearly seen in the analysis of individual CL frequencies binned by proxy values. If ~~CL0~~ noCL is excluded, all ELF/LTS/EIS have good inter-CL correlations with the amount-when-present (AWP) of individual CLs. In future, an advanced ELF needs to be formulated to deal with the ~~dissipation~~ decrease of LCA when the inversion base height is lower than the lifting condensation level, to diagnose cumulus updraft fraction as well as the amount of stratiform clouds and detrained cumulus, and to parameterize the scale height as a function of appropriate environmental variables.

1 Introduction

During the ~~last decade~~past few decades, there have been extensive efforts to quantify the impact of low-level clouds on the Earth's climate. However, despite its important role in the global radiation budget and hydrological cycle, various cloud-related feedback processes are not well represented in most general circulation models (GCMs). Because the climate sensitivities of GCMs are strongly dependent on the representation of cloud processes (e.g., Cess et al. (1990), Stephens (2005), Bony and Dufresne (2005), Andrews et al. (2012), Nam et al. (2012), and Brient and Bony (2012)), the correct understanding and accurate parameterizations of cloud processes are critical for the successful simulation of the Earth's future climate.

Numerous studies have attempted to understand the complex physics and dynamic processes controlling the formation and dissipation of marine stratocumulus clouds (MSC) through observational analysis and modeling (see Wood (2012)). Using large-scale environmental variables, several studies have endeavored to find a simple proxy that can diagnose spatial and

temporal variations in MSC. Klein and Hartmann (1993) (KH93 hereafter) showed that a lower tropospheric stability, LTS$\equiv \theta_{700} - \theta_{1000}$ where θ_{700} and θ_{1000} are the potential temperatures at 700 and 1000 hPa levels, respectively, well correlates with the seasonal variations in LCA in the subtropical marine stratocumulus deck. The observed empirical relationship between LTS and subtropical LCA was used to parameterize LCA in some GCMs (Slingo (1987); Collins et al. (2004)) or evaluate GCMs (Park et al., 2014). Based on the decoupling hypothesis (e.g., Augstein et al. (1974), Albrecht et al. (1979), Betts and Ridgway (1988), Bretherton (1992), and Park et al. (2004)), Wood and Bretherton (2006) (WB06 hereafter) suggested an estimated inversion strength (EIS) as an alternative proxy for LCA in the subtropical and midlatitude marine stratocumulus decks. Although uncertainty exists regarding whether the observed relationship between EIS and LCA still maintains in future climate, EIS has been used to predict the variations in LCA in response to the climate changes (Caldwell et al. (2013), Qu et al. (2014, 2015)). More recently, Kawai et al. (2017) proposed an estimated cloud-top entrainment index (ECTEI) as a proxy for MSC, which is a modified EIS that takes into account a cloud-top entrainment criteria.

Although the aforementioned proxies (i.e., LTS, EIS, and ECTEI) have been shown to be extremely useful in diagnosing the variations in MSC over the subtropical and midlatitude oceans, their applicability in the other regions (e.g., lands, tropics, and high latitude regions) has been in question (in this regard, it may be more reasonable to interpret LTS/EIS as one of the cloud-controlling factors rather than a proxy for LCA). Park and Shin (2019) (PS19 hereafter) found that these proxies are not strongly correlated with the observed LCA when the analysis domain is extended over the entire globe and suggested an estimated low-level cloud fraction (ELF) as a new proxy for the analysis of the spatiotemporal variations in the global LCA. ELF is defined as ELF=$f \cdot (1 - \sqrt{z_{LCL} \cdot z_{inv}}/\Delta z_s)$, where $f = max[0.15, min(1, q_{v,ML}/0.003)]$ is a freezedry factor with the water vapor specific humidity in the surfaced-based mixed layer, $q_{v,ML}$ in [g kg^{-1}]; z_{LCL} is the lifting condensation level (LCL) of near-surface air; z_{inv} is the inversion height estimated from the decoupling hypothesis suggested by Park et al. (2004); and $\Delta z_s = 2750\ [m]$ is a constant scale height. PS19 showed that ELF is superior to LTS, EIS, and ECTEI in diagnosing the spatial and temporal variations in the seasonal LCA over both the ocean and land, including the marine stratocumulus deck, and explains approximately 60% of the spatial-seasonal-interannnual variance of the seasonal LCA over the globe, which is a much larger percentage than those explained by LTS (2%) and EIS (4%). PS19 also noted several weaknesses of ELF, such as its tendency to underestimate LCA over the deserts and North Pacific and Atlantic oceans and overestimate LCA in other regions.

In this study, we extend PS19 and examine the relationship between LCA and its proxies by individual low-level cloud types. Individual low-level cloud has its own distinct structure of the planetary boundary layer (PBL) and synoptic environmental conditions (Norris (1998), Norris and Klein (2000)). As the PBL transitions from the well-mixed to a decoupled state, surface-observed low-level clouds change from stratocumulus (CL5 where CL is a low-level cloud code used by surface observers defined from WMO (1975a); see also Park and Leovy (2004)) to cumulus-under-stratocumulus (CL8) and stratocumulus formed by the spreading out of cumulus (CL4), and eventually to shallow (CL1), moderate (CL2), and precipitating deep cumulus (CL3) with an anvil (CL9). In the stable PBL, sky-obscuring fog (CL11) or fair weather stratus (CL6) are likely to be observed when the inversion height is slightly higher than z_{LCL} but low-level cloud cannot be formed (CL0) if the inversion height is lower than z_{LCL}. In general, fractional area covered by stratiform clouds is larger than that of convective clouds. It is

expected that a detailed analysis of the relationship between LCA and various proxies by individual CLs will provide insights regarding the sources of the strengths and weaknesses of various proxies, which may help to develop a better proxy for LCA.

The structure of this paper is as follows. Section 2 briefly explains the conceptual framework of ELF including the data and analysis methods. Section 3 shows the results of the analysis of climatology and seasonal cycle of various CLs and the relationship between the amount-when-present (AWP), frequency (FQ), and amount (AMT) of individual CL and various proxies. Several ways to develop an advanced ELF in future is also discussed. A summary and conclusion are provided in Section 4.

2 Method

2.1 Conceptual Framework

PS19 provided a detailed description of the definition and physical meaning of various proxies for LCA, which are briefly summarized here. The lower-tropospheric stability (LTS) and estimated inversion strength (EIS) are defined as

$$LTS \equiv \theta_{700} - \theta_{sfc}, \tag{1}$$

$$EIS = LTS + \Gamma^m_{LCL} \cdot z_{LCL} - \Gamma^m_{700} \cdot z_{700}, \tag{2}$$

where θ_{700} and θ_{sfc} are the potential temperatures at 700 [hPa] and surface, respectively, and Γ^m_{LCL} and Γ^m_{700} are the moist adiabatic lapse rates of θ (in unit of $[K \cdot m^{-1}]$) at the lifting condensation level of near surface air (z_{LCL}) and 700 [hPa] height (z_{700}), respectively. The estimated cloud-top entrainment index (ECTEI, Kawai et al. (2017)) is defined as

$$ECTEI = EIS - \beta(L_v/c_p)(q_{v,sfc} - q_{700}), \tag{3}$$

where $\beta = 0.23$, L_v is the latent heat of vaporization, c_p is the specific heat at constant pressure, and q_{700} is the specific humidity at 700 hPa.

The estimated low-level cloud fraction (ELF) is defined as

$$ELF \equiv f \cdot \left[1 - \frac{\sqrt{z_{inv} \cdot z_{LCL}}}{\Delta z_s}\right] = f \cdot \left[1 - \beta_2\right], \tag{4}$$

where $\beta_2 = \sqrt{z_{inv} \cdot z_{LCL}}/\Delta z_s$ is a low-level cloud suppression parameter with a constant scale height $\Delta z_s = 2750\ [m]$, z_{inv} is the inversion height,

$$\begin{aligned} z_{inv} &= -\left(LTS/\Gamma^m_{700}\right) + z_{700} + \Delta z_s \cdot \left(\frac{\Gamma^m_{LCL}}{\Gamma^m_{700}}\right) \\ &= -\left(EIS/\Gamma^m_{700}\right) + z_{LCL} \cdot \left(\frac{\Gamma^m_{LCL}}{\Gamma^m_{700}}\right) + \Delta z_s \cdot \left(\frac{\Gamma^m_{LCL}}{\Gamma^m_{700}}\right), \quad z_{LCL} \le z_{inv} \le z_{LCL} + \Delta z_s, \end{aligned} \tag{5}$$

and f is the freezedry factor (Vavrus and Waliser, 2008) defined as a function of water vapor specific humidity at surface ($q_{v,sfc}$ in unit of $[g \cdot kg^{-1}]$),

$$f = max\left[\, 0.15,\ min\left(1,\ \frac{q_{v,sfc}}{0.003}\right)\,\right],. \tag{6}$$

~~and z_{inv} is the inversion height,~~

~~$z_{inv} = -\left(LTS/\Gamma^m_{700}\right) + z_{700} \qquad + \Delta z_s \cdot \left(\frac{\Gamma^m_{LCL}}{\Gamma^m_{700}}\right)$~~

$$= -\left(EIS/\Gamma^m_{700}\right) + z_{LCL} \cdot \left(\frac{\Gamma^m_{LCL}}{\Gamma^m_{700}}\right) + \Delta z_s \cdot \left(\frac{\Gamma^m_{LCL}}{\Gamma^m_{700}}\right),$$

~~where $\Delta z_s = 2750\ [m]$ is a constant scale height.~~

Using the decoupling hypothesis of PLR04, PS19 estimated z_{inv} by assuming that the decoupling parameter α can be parameterized as a linear function of the decoupled layer thickness, $\Delta z_{DL} \equiv z_{inv} - z_{LCL}$,

$$\alpha \equiv \frac{\theta^-_{inv} - \theta_{sfc}}{\theta^+_{inv} - \theta_{sfc}} \approx \left(\frac{\Delta z_{DL}}{\Delta z_s}\right), \quad 0 \le \alpha \le 1, \tag{7}$$

where $\theta^+_{inv} = \theta_{700} - \Gamma^m_{700} \cdot (z_{700} - z_{inv})$ and $\theta^-_{inv} = \theta_{sfc} + \Gamma^m_{LCL} \cdot (z_{inv} - z_{LCL})$ are the potential temperatures just above and below the inversion height (see Fig. 1 of PS19). In deriving ELF, it was assumed that the top of surface-based mixed layer is identical to z_{LCL}. The freezedry factor is designed to reduce the parameterized cloud fraction in the extremely cold and dry atmospheric conditions typical of polar and high latitude winters. ELF can be also written as ELF=$f \cdot [\ 1 - (z_{LCL}/\Delta z_s)\sqrt{1 + (z_{inv} - z_{LCL})/z_{LCL}}\ ]$, where f ~~denotes~~ is an increasing function of the amount of water vapor in the surface air, z_{LCL} represents the degree of subsaturation of near-surface air, and $(z_{inv} - z_{LCL})/z_{LCL}$ quantifies the degree of thermodynamic decoupling of the inversion base air from the surface air. ELF predicts that LCA increases as the near-surface air becomes more saturated with enough amount of water vapor and as the PBL becomes more vertically coupled, which is consistent with what is expected to happen in nature. To ensure $0 \le \alpha \le 1$ (i.e., thermodynamic scalars at the inversion base (θ^-_{inv}) are bounded by the surface (θ_{sfc}) and inversion top (θ^+_{inv}) properties), the inversion height computed from Eq.(5) was forced to satisfy $z_{LCL} \le z_{inv} \le z_{LCL} + \Delta z_s$.

2.2 Data and Analysis

The data used in our study are identical to that used in PS19. The surface observation data are from the Extended Edited Cloud Report Archive (EECRA, Hahn and Warren (1999)), which compiles individual ship and land observations of clouds, present weather, and other coincident surface meteorologies every 3 or 6 hours. The upper-level meteorologies (e.g., p and θ) are from the ERA interim reanalysis products (ERAI, Simmons et al. (2007)) at 6-hourly time intervals. Spatial and temporal interpolations are performed to compute the upper-level meteorologies at the exact time and location at which the EECRA surface observers reported the LCA. Our analysis uses the data from January 1979 to December 2008 (30 years) over the

ocean and January 1979 to December 1996 over land (18 years). Using the 6-hourly ERAI vertical profile of θ and water vapor interpolated to individual EECRA surface observations, we computed ~~the seven proxies for LCA (i.e., LTS, EIS, ECTEI, ELF,~~ α, z_{LCL}, and z_{inv}~~)~~.

The surface observer reports cloud type (CL) and fractional area (LCA) of low-level clouds following a strict hierarchy from the World Meteorological Organization (WMO (1975b). Table 1). In addition to the ten CL types defined by WMO, EECRA defines two more CL types (CL10, sky-obscuring thunderstorm and shower, and CL11, sky-obscuring fog) by combining the present weather code with the observation of missing CL. Consequently, an individual EECRA observation contains 12 CLs (from CL0 to CL11) and associated LCA (from 0 to 8 octa), such that a set of 12 CLs forms a complete basis function for the entire EECRA data. Based on similarities in morphology and physical property, we grouped individual CLs into the eight groups: ~~CL0, CL11, CL6, CL7, CL5, CL84 (Cumulus-with-Stratocumulus), CL12 (Cumulus~~noCL (no low-level cloud), Fog (sky-obscuring fog), F.St (fair weather stratus), B.St (bad weather stratus), Sc (stratocumulus), Sc-Cu (stratocumulus and cumulus), Cu (cumulus), and ~~CL39 (Cumulonimbus~~Cb (cumulonimbus), in approximately the increasing order of vertical instability ~~.~~ (see Table 2). Since ELF is based on the decoupling hypothesis that can be applied in various regimes from the well-mixed to fully decoupled states, we included all CLs in our analysis. For individual CLs or combinations of CLs, we computed cloud frequency (FQ), amount-when-present (AWP), and amount (AMT), following the procedures described in Hahn and Warren (1999) and Park and Leovy (2004). Cloud FQ for a specific CL is defined by the fraction of observations reporting the specific CL among the total set of observations reporting any CL information. Cloud AWP is the average LCA when a specific CL is observed. Cloud AMT is the product of FQ and AWP.

Similar to PS19, individual EECRA cloud observations, surface and upper-level meteorologies are averaged into 5^olatitude x 10^olongitude seasonal data for each year. To reduce the impact of random noise, a minimum of 10 observations were required to form effective seasonal grid data in each year. These seasonal grid data are used for computing annual climatologies and seasonal differences of various CLs (Fig. ~~1~~1-2) and analyzing correlations between the LCA and various proxies by cloud types (Tables 1-2 and Figs. ~~2-5~~3-6). In addition, individual EECRA cloud observations are grouped into bins of individual proxies to better understand the contribution of individual CLs to the overall correlation relationship between the proxies and LCA (Figs. ~~6-7~~7-8). ECTEI produced results very similar to those of EIS, such that only the analysis from EIS are shown in this study.

3 Results

3.1 Climatology and Seasonal Cycle

~~Figure~~ Figures 1 ~~shows~~ and 2 show the annual climatology and the differences in the seasonal FQ of various CLs during JJA and DJF. ~~CL0~~ As shown, noCL is frequently observed over the continents but is rarely reported over the open ocean, implying that ~~primary factor~~ one of the important factors controlling the formation of low-level clouds is the moisture source at the surface. One of the rare open ocean areas with annual ~~CL0~~ noCL FQ larger than 10% is the sea surface temperature (SST) cold tongue region in the eastern equatorial Pacific ocean, where SST is lower than the overlying air temperature, net upward buoyancy flux from the sea surface is very weak, and atmospheric PBL is stable (Deser and Wallace, 1990). As a result,

turbulent vertical moisture transport from the sea surface to z_{LCL} is strongly suppressed (i.e., $z_{inv} < z_{LCL}$), resulting in the maximum FQ of ~~CL0~~ noCL (Park and Leovy, 2004). This indicates that not only the moisture source at the surface, but also vertical stability in the atmospheric PBL controls the formation of low-level clouds. Over the continents and the Arctic area, ~~CL0~~ noCL is more frequently observed during boreal winters than summers, presumably because strong daytime insolation during summer destabilizes the lower troposphere, promoting the onset of convective clouds (i.e., ~~CL84, CL12, and CL39), strong~~ Sc-Cu, Cu, and Cb). Strong nocturnal LW radiative cooling during winter stabilizes the lower troposphere, ~~forcing~~ which forces $z_{inv} < z_{LCL}$~~, and~~ . In addition, the amount of moisture at the near surface is very small during winter. Similar to the case over the SST cold tongue, strong vertical stability over the winter continents and Arctic area appears to increase the probability of the occurrence of ~~CL0~~noCL, which appears to be somewhat opposite to the embedded decoupling processes into ELF that increases as z_{inv} decreases. However, with the freezedry factor, ELF may be able to capture enhanced ~~CL0~~ noCL frequency over the continents during winter due to a small amount of moisture near the surface. This is because the freezedry factor substantially reduces ELF in this region during winter as shown in PS19.

~~CL11~~ Fog is frequently observed over the western North Pacific and Atlantic oceans, including the Arctic area, during JJA when the Arctic sea ice melts and moist warm airs are advected into cold SST region across the midlatitude SST front. This indicates the saturation of advected air parcels by the contact cooling with the underlying cold SST or more upward moisture transport from the open ocean over the Arctic, which can be captured by ELF through the decrease in z_{LCL}. ~~CL6~~ F.St has a similar climatology and seasonal cycles as ~~CL11~~Fog, implying that the physical processes controlling the formation of ~~CL11~~ Fog are similar to those of ~~CL6.CL7~~ F.St. B.St has an annual climatology similar to that of ~~CL6~~ F.St but its seasonal cycle over the North Pacific and Atlantic oceans is opposite to that of ~~CL6~~F.St, with more frequency during boreal winters. Similar to ~~CL7, CL39~~ B.St, Cb is more frequently observed during winter in this region, which is presumably due to the frequent passage of midlatitude synoptic storms in winter. A composite analysis showed that ~~CL39~~ Cb is frequently observed on the rear side of the midlatitude synoptic cold front with a reduced lower tropospheric stability, while ~~CL7~~ B.St is observed on the front or near center of synoptic storm with an enhanced lower tropospheric stability ~~(not shown)~~(Park and Shin, 2020). When the midlatitude storm track passes, anomalous mean vertical motion in the mid-troposphere drives the changes in the mid-level clouds, but the variations in the lower tropospheric stability also drive the changes of LCA, which can be captured by ELF through the variations in z_{inv}.

~~CL5 is more~~ In the northern hemisphere, Sc is frequently observed over the eastern subtropical and midlatitude oceans during JJA, when the subtropical and midlatitude high is strong and the PBL is relatively well coupled. In the Namibian and Peruvian stratocumulus decks west of the South America and South Africa, Sc is most frequently reported during SON when SST is at a minimum (Klein and Hartmann, 1993). Over most ocean areas, seasonal variations in ~~CL5~~ Sc tend to be opposite to those of ~~CL12 and CL39~~Cu and Cb. ELF is designed to capture these conversions between ~~CL5 and CL12~~ Sc and Cu in association with the PBL decoupling. Over northern Asia and Canada, including a portion of the Arctic area, both convective and stratiform clouds are more frequently observed during boreal summers than winters, presumably due to the destabilization of the lower troposphere by strong insolation heating and more surface moisture.

3.2 Proxy vs the AWP of Individual Low-Level Clouds

Figures ~~2 and~~ 3 and 4 show the composite anomalies of LCA and various proxies with respect to the seasonal climatology when a specific CL was reported (see Figs. S1 and S2 for the composite anomalies of z_{LCL}, z_{inv}, α, and $1-\beta_2$). The anomalous LCA in the top row (ΔAWP) is the difference between the amount-when-present (AWP) when a specific CL was reported, and climatological LCA. To examine the coherency between ΔAWP and the anomalies of individual proxies in each grid box, we computed the non-centered geographical correlation coefficients between ΔAWP and ΔProxy over the entire globe (G), ocean (O) and land (L), respectively, which are shown at the top of the individual plots. Here, we used the non-centered correlations rather than centered correlations to assess whether the spatial means of ΔAWP and ΔProxy, as well as the spatial variabilities of those, are similar.

When ~~CL0~~ noCL is reported, AWP is zero, that is, ΔAWP = $-$LCA in Fig. ~~2a~~3a. However, both LTS and EIS increase (G=-0.71 and -0.62 for LTS and EIS, respectively), particularly over the far northern continents and Arctic area. This is because noCL can occur when inversion is strong near the surface under dry conditions (Norris, 1998; Koshiro and Shiotani, 2014). Conversely, ELF decreases in a desirable way, due to the freezedry factor (compare Fig. ~~2y with 2~~3m with Fig. S1m). Over the eastern subtropical marine stratocumulus deck, all LTS/EIS/ELF show a hint of negative anomaly which, however, is too weak to explain the substantial decrease in LCA when ~~CL0~~ noCL is reported. Over the midlatitude oceans, the situation is worse and none of the factors comprising ELF (i.e., z_{LCL}, z_{inv}, and α) can explain the decrease in LCA ~~.~~ (Figs. S1a, e, i). Although slightly better than LTS and EIS, ELF has an apparent problem in diagnosing the decrease of LCA when ~~CL0~~ noCL was reported, particularly over the ocean (O=0.15). This problem worsens without the freezedry factor (Fig. ~~2y~~S1m). When ~~CL11, CL6, or CL7~~ Fog, F.St, or B.St are reported, LCA increases over the entire globe, which are very well captured by ELF (G=0.97, 0.89, and 0.88 for ~~CL11, CL6, and CL7~~Fog, F.St, and B.St, respectively), due to the simultaneous decreases in z_{LCL}, z_{inv}, and α. Although slightly worse than ELF, LTS and EIS also captures the increase of LCA when ~~CL11~~ Fog was reported (G=0.85 and 0.44 for LTS and EIS, respectively). However, undesirable negative anomalies of LTS and EIS over the far northern continents including Arctic area get worse from ~~CL11 to CL6 and CL7~~Fog to F.St and B.St, resulting in very weak (G=0.17 for LTS) or even negative (G=-0.43 for EIS) correlations between ΔLTS/ΔEIS and ΔAWP when ~~CL7~~ B.St was reported. We speculate that in these dry regions, the formation of Fog, F.St, and B.St needs upward moisture transports from the surface, which is likely to be accompanied by the reduction of vertical stability in the lower troposphere (e.g., breakup of sea-ice over the Arctic). As a result, ΔLTS/ΔEIS are negatively correlated with ΔAWP over the far northern continents and Arctic area. Overall, ELF is better than LTS and EIS in diagnosing the variations of fog and stratus over both the ocean and land. It should be noted that LTS, EIS, and ECTEI are mainly designed to be used over the ocean without sea ice and they are not intended to be used over land and sea ice.

In addition to the fog and stratus, ELF captures the variations in LCA in association with ~~CL5~~ Sc (G=0.74), ~~CL84~~ Sc-Cu (G=0.52), ~~CL12~~ Cu (G=0.31), and ~~CL39~~ Cb (G=0.62) reasonably better than LTS and EIS. When ~~CL5~~ Sc was reported and so LCA increases, both LTS and EIS increase over the subtropical and midlatitude oceans. However, over the Arctic, Asia, and deserts areas, LTS/EIS shows negative anomalies opposite to the increased LCA, which worsens and extends to other continents

from ~~CL5, CL84 to CL12 and CL39~~Sc, Sc-Cu to Cu and Cb, resulting in substantial negative correlations between ΔLTS/ΔEIS and ΔLCA over land for ~~CL84~~ Sc-Cu (L=-0.65/-0.71 for LTS/EIS), ~~CL12~~ Cu (L=-0.38/-0.38), and ~~CL39~~ Cb (L=-0.74/-0.80). The negative correlation for Sc can be explained by the same physical processes applied to the cases of Fog, F.St, and B.St as explained above (i.e., enhanced moisture transport from the surface and associated decrease in vertical static stability). In the very dry regions where background LCA is very small, the onset of Cu and Cb in unstable situations (e.g., decreases of LTS/EIS) will result in the increase of LCA. Although generally better than LTS/EIS, ELF also has a problem in capturing the increase in LCA over Asia and most desert areas when ~~CL12~~ Cu was reported (L=-0.14). In summary, an advanced ELF in future should be designed to capture the decrease in maritime LCA associated with ~~CL0~~ noCL and the increase in continental LCA associated with ~~CL12~~Cu.

Figure ~~4~~ 5 shows the area-averaged seasonal climatology of the AWP and various proxies when a specific CL was reported over the ocean and land during the daytime (9 am - 9 pm) and nighttime (9 pm - 9 am), respectively (see Fig. S3 for z_{LCL}, z_{inv}, α, and $1-\beta_2$). By definition, ~~CL11~~ Fog is always overcast and stratiform clouds tend to have larger AWP than convective clouds. ~~CL39~~ Cb has larger AWP than ~~CL12~~Cu, presumably due to larger cross-sectional/lateral areas of deep convective updraft plumes or the contribution of detrained convective condensates. With the exception of ~~CL39~~Cb, AWP over the ocean is slightly larger than that over land. The diurnal cycle of the AWP in most CLs is very weak. However, continental ~~CL39~~ Cb during the night tends to have a slightly larger AWP than during the day, which seems to be contradictory to intuition that deep cumulonimbus over land is forced by strong insolation heating during the day. This may reflect the late evening or nocturnal development of the strongest deep convective system over the continents in association with the gradual buildup of the mesoscale convective organization forced by the evaporation of convective precipitation (Park (2014a, b)). As a global proxy for the AWP of individual CL, ELF shows more desirable inter-CL variations than LTS and EIS, which have strong ocean-land contrasts (in particular, EIS) and seasonal cycle over land. The weaker seasonal cycle and ocean-land contrasts of ELF may imply the opposite variations in z_{inv} and z_{LCL}. Due to the freezedry factor, ELF is slightly smaller than $1-\beta_2$ during DJF over land~~.~~, and the freezedry factor also contributes to reducing the excessive seasonal cycle (compare Fig. 5h and Fig. S3h). ELF has a somewhat stronger diurnal cycle than AWP over land with a larger ELF during the night, which is presumably due in part to diagnosing the noCL condition as a non-zero ELF, as will be explained later. The factors comprising ELF (z_{LCL}, z_{inv}, and α) have fairly similar inter-CL variations with larger values for convective than stratiform clouds ~~.~~(Fig. S3). Interestingly, z_{LCL} for ~~CL39~~ Cb is smaller than that of ~~CL12~~Cu, presumably due in part to the evaporation of convective precipitation and associated moistening and latent cooling of near surface air when ~~CL39~~ Cb was reported.

Figure ~~5~~ 6 shows the scatter plots of individual CL's AWP as a function of LTS, EIS, 1-β_2, and ELF obtained from Fig. ~~4. If CL0~~ 5. If noCL is excluded, all proxies have very good correlations with the AWP of individual CLs, although ELF and $1-\beta_2$ perform slightly better than LTS and EIS. ~~In the case of EIS over land, the regression lines seem to be slightly offset from the data scatters with seemingly too high~~ If Fog is also excluded, the correlations between LTS/EIS and AWP are substantially degraded, whereas the performances of ELF and $1-\beta_2$ do not change much (see R^2 ~~, which is due to CL11 in DJF that has a high EIS located outside of the plotting range.~~ in the parenthesis of Fig. 6). Similar to the regression analysis of PS19, the slope of inter-CL AWP regressed on ELF during the day over the ocean is steeper than that over land. Over the ocean, the

regression slopes during the night are roughly similar to those during the day but with systematically higher proxy values. For all cloud types, ELF during the night tends to be larger than during the day, particularly over land, indicating that the product of z_{inv} and z_{LCL} during the day is larger than during the night. This is an anticipated result since shortwave radiative heating of the surface during the day destabilizes the lower troposphere (i.e., increases z_{inv}) and decreases the relative humidity of the near surface air (i.e., increases z_{LCL}). Over land, however, both ELF and $1-\beta_2$ tend to have steeper regression slopes during the night than during the day. This is due in part to the diagnosis of noCL condition as a non-zero ELF, particularly during the night, when noCL conditions are frequently reported (see Fig. 1a). To be a better proxy for LCA (i.e., LCA=ELF denoted by the dashed grey line), ELF of ~~CL0 (and CL12~~ noCL (and Cu except over land during the day) should be much lower than the current values, while the ELFs of ~~CL5, CL84, CL39 and CL12~~ Sc, Sc-Cu, Cb and Cu over land during the day as well as ~~CL11 and CL67~~ Fog, F.St, and B.St over the ocean should be higher than the current values. These required behaviors are fairly consistent with the conclusion drawn from the analysis of Figs. ~~2 and 3.~~ 3 and 4. In contrast to previous studies reporting a superior performance of EIS to LTS, our analysis does not show a clear difference in their performances. This is presumably because our study compared their performances over the entire globe instead of marine stratocumulus decks, the main target areas of EIS and LTS.

3.3 Proxy vs the FQ of Individual Low-Level Clouds

Figure ~~6 is the cumulative~~ 7 is the stacked percentage plot of the frequencies of individual CLs in the bins of various proxies, defined as the number of observations reporting a specific CL type divided by the total observation number in each bin. Figure ~~6a~~7a, a plot with a perfect proxy for LCA, shows that ~~CL0~~ noCL exists entirely in the zero octa bin, ~~CL11~~ Fog only exists in the 8 octa bin, and the bin AWP (black line) increases in a perfect linear way as LCA increases, as expected. As LCA increases, the frequency of ~~CL12~~ Cu decreases but those of stratiform clouds (~~CL6, CL7, CL5 and CL84~~F.St, B.St, Sc, and Sc-Cu) tend to increase. In contrast to ~~CL12~~Cu, the frequency of ~~CL39~~ Cb in the low octa bins gradually increases with LCA. The observation number is relatively large in the zero and 8 octa bins (yellow line). The low-level cloud AMT contributed by individual bin (the cyan line that is a simple product of the black and yellow lines) increases with LCA but not in a perfectly linear way. The overall patterns over land are approximately similar to those over the ocean. Over land, the observation number is the largest in the zero octa bin and convective clouds (~~CL12 and CL39~~Cu and Cb) are mostly observed during the day. Any good proxy for LCA, if any, should have similar patterns as Figs. ~~6a~~ 7a and b.

The frequency of ~~CL0~~ noCL increases as LTS and EIS increase, which is mainly responsible for the undesirable decreases in the AWP and AMT in the high bins of LTS and EIS. Designed as a proxy for marine stratocumulus, however, LTS/EIS reasonably simulates the increase (decrease) in ~~CL5 (CL12~~Sc (Cu) frequency with LTS/EIS over the ocean. The increase of noCL frequency with LTS/EIS seems to be contradictory to our simple intuition that LTS/EIS is positively correlated with LCA. However, we note that noCL condition is frequently reported with a strong inversion near the surface when LTS/EIS is large (Norris, 1998; Koshiro and Shiotani, 2014). Note that the implied correlation between LCA and EIS in Fig. 7e is weaker than the previous studies (Wood and Bretherton, 2006), since LCA in Fig. 7 is defined by including all low-level cloud types over the globe. In contrast to the case of LCA, ~~CL11~~ Fog exists in several bins and the frequency of ~~CL39~~ Cb decreases

monotonically with LTS/EIS. Similar to the case of LTS/EIS, ~~CL0~~ noCL exists ubiquitously in the entire ELF bins, indicating that ~~LTS/EIS/ELF frequently diagnoses~~ the observed noCL conditions are frequently misinterpreted as cloudy conditions with LTS/EIS/ELF. However, the frequency of ~~CL0~~ noCL tends to decrease with ELF, such that the bin AWP increases in a desirable way as ELF increases, although the slope is smaller than the case of LCA. The frequency of ~~CL0~~ noCL in the nonzero ELF bins over land is substantially higher than that over the ocean. The observation number FQs in the zero and 8 octa ELF bins are substantially lower than those in the LCA bins but higher in the intermediate bins, implying that an advanced ELF needs to transfer the observation number FQ in the intermediate ELF bins into the zero octa bin (e.g., by correctly diagnosing ~~CL0~~ noCL condition) and 8 octa bin (e.g., by correctly diagnosing ~~CL11~~ Fog condition).

Table ~~2~~ 3 shows spatial-seasonal correlation coefficients between the frequency of individual CL and various proxies. In contrast to Figs. ~~2~~ 3 and 4, Table 3 ~~, Table 2~~ (also Table ~~3~~4) shows a conventional centered-correlation between the seasonal climatologies (i.e., averaged over all observations) of various proxies and individual CL frequency. LCA increases as the frequencies of sky-obscuring fog (~~CL11~~Fog), stratus (~~CL6, CL7~~F.St, B.St), stratocumulus (~~CL5, CL84~~Sc, Sc-Cu), and continental convective clouds (~~CL12, CL39~~Cu, Cb) increase, and decreases as the frequencies of ~~CL0~~ noCL and marine convective clouds increase. Except for marine ~~CL84 and continental CL12~~Sc-Cu and continental Cu, ELF reproduces these correlation characteristics of LCA with individual CL well, at least qualitatively. The freezedry factor substantially contributes to the improved correlations of ~~CL0~~ noCL with ELF from β_2. As explained in PS19, the freezedry factor ($f = max[\,0.15,\ min(1,\ q_{v,sfc}/0.003)\,]$) is designed to reduce a diagnosed LCA in a very dry region, such that it is most effective over the far northern continents and Arctic area, particularly during winter. Over the globe, ~~CL0~~ noCL is negatively correlated with z_{inv} and α (not shown), presumably due in part to the frequent occurrence of ~~CL0~~ noCL on the west coast of the major continents and equatorial SST cold tongue regions where z_{inv} is low due to cold SST ~~.~~ (see Fig. 1a). The frequent occurrence of noCL on the west coast is due to the advection of dry air from nearby continents (Mansbach and Norris, 2007). The frequent occurrence of noCL over the SST cold tongue is due to the warm air advection from the south and associated stabilization of the lower PBL and suppression of vertical moisture transport from the sea surface to z_{LCL} (Park and Leovy, 2004). Designed as a proxy for marine stratocumulus, LTS/EIS show a strong correlation with ~~CL5~~ Sc FQ over the ocean. However, the correlation characteristics of LTS/EIS with other CLs are less desirable than that of ELF. For example, the correlations of LTS/EIS with ~~CL11, CL6, and CL7~~ Fog, F.St, and B.St over the globe and continental ~~CL5~~ Sc are significantly weaker than those of LCA and the correlation signs with ~~CL0, CL84~~noCL, Sc-Cu, and continental ~~CL12 and CL39~~ Cu and Cb are opposite to those of ELF and LCA. One of the most ~~undesirable~~ unexpected aspects of LTS and EIS is a strong positive correlation with ~~CL0~~ noCL FQ, as was shown in Fig. ~~6.~~ 7. This may indicate a non-linear response of clouds to the inversion strength or the existence of other factors controlling the onset of noCL condition.

3.4 Proxy vs the AMT of Individual Low-Level Clouds

Figure ~~7 is the cumulative~~ 8 is the stacked plot of the AMT of individual CLs in the bins of various proxies. The LCA is the AMT of all CLs. The bin cloud AMT (the cyan line) increases monotonically with LCA with the largest increase from the 7 to 8 octa-bin (Fig. ~~7a~~8a, b). In the low bins, convective clouds contribute to the cloud AMT more than stratiform clouds but in the

high bins, stratiform clouds contribute more. Total cloud AMT (i.e., the integration of the cyan line across the entire bins) over the ocean is larger than that over land. In the 8 octa bin over land, ~~CL39~~ Cb contributes more than 20% to the cloud AMT. In contrast to LCA, none of the proxies show a required monotonic increase in the bin cloud AMT. Over the ocean, EIS shows an undesirable monotonic decrease in the bin cloud AMT, LTS is slightly better than EIS, and ELF shows a further improvement with the maximum bin cloud AMT shifting to the higher bin. The improvement from EIS/LTS to ELF is more pronounced over land but the rapid decrease in bin cloud AMT from the 7 to 8 octa ELF bins is problematic. These variations in the bin cloud AMT are largely controlled by the variations in the bin cloud FQ (see the yellow line in Fig. ~~6~~7). All proxies show the increase in the relative contribution of stratiform clouds to the bin cloud AMT as the bin value increases but the contribution of ~~CL39~~ Cb AMT in the 8 octa bin over land is smaller than that of LCA.

Table ~~3~~ 4 shows spatial-seasonal correlation coefficients between the AMT of individual CL and various proxies. The overall correlation characteristics of the cloud AMT are very similar to those of the cloud FQ shown in Table ~~2.~~ 3. LCA tends to increase as the cloud AMT of individual CL increases. The only exception is marine ~~CL12~~ Cu AMT that decreases as LCA increases. ELF reproduces these correlation characteristics of the AMT of individual CL with LCA well. As a global proxy for LCA, the correlation characteristics of LTS/EIS with individual cloud AMT are less desirable than that of ELF: the correlations with continental ~~CL12 and CL84~~ Cu and Sc-Cu are unrealistically negative and the correlations with sky-obscuring fog and stratus are much weaker than those of ELF and LCA. ~~Table 3~~ We note that LTS, EIS, and ECTEI are designed to be used over the ocean without sea ice, and they are not intended to be used over land and sea ice. Table 4 indicates that a superior performance of ELF to LTS/EIS as a global proxy for LCA discovered by PS19 (see the bottom row of Table ~~3~~4) is derived from its realistic correlations with various CLs rather than with a specific CL.

3.5 What ~~are~~ is necessary to further improve ELF as a global proxy for LCA ?

We have shown that generally, ELF diagnoses the inter-CL variations in LCA better than LTS/EIS. However, we also identified several weaknesses in ELF, such as the increase in ELF over the ocean when ~~CL0~~ noCL was reported, and the decrease in ELF over the deserts and Asian continents when ~~CL12~~ Cu was reported and so LCA increases. In this section, we examine in more details why ELF shows undesirable correlations with LCA for some cases and then provide a potential pathway to further improve ELF in future.

When ~~CL0~~ noCL is reported, ELF increases over the North Pacific and North Atlantic oceans, which results in a very weak non-centered correlation over the ocean (O=0.15) between ΔLCA (Fig. ~~2a~~3a) and ΔELF (Fig. ~~2~~3m). Although the correlation over land (L=0.65) is higher than over the ocean, the magnitude of ΔELF is much smaller than ΔLCA. As shown in Figs. ~~5g and 5h, CL0~~ 6g and 6h, noCL is the most distinct outlier from the desirable AWP=ELF line (dashed lines) in the inter-CL scatter plots. This mis-diagnosis of ~~CL0~~ noCL condition with non-zero ELF is also shown in Figs. ~~6i and 6j~~ 7i and 7j and it worsens over land during the night. To understand this problem, we plotted the probability density function (PDF) of $z_{DL} \equiv z_{inv} - z_{LCL}$ using individual observations reporting ~~CL0~~ noCL and compared it with the PDF of entire observations (CLM) over the ocean (Fig. ~~8a~~9a) and land (Fig. ~~8b~~9b), respectively. As shown, the PDF of near zero z_{DL} when ~~CL0~~ noCL was reported is higher than that of CLM and the difference over land is larger than that over the ocean. Conceptually, if

$z_{DL} < 0$ and so $z_{inv} < z_{LCL}$, low-level cloud cannot be formed, such that LCA is likely to be small. This can happen when dry air at the surface is capped by a strong inversion, such that vertical moisture transport from the surface to z_{LCL} is inhibited. However, since our ELF= $f \cdot (1 - \sqrt{z_{inv} \cdot z_{LCL}}/\Delta z_s) = f \cdot [\, 1 - (z_{LCL}/\Delta z_s)\sqrt{1 + z_{DL}/z_{LCL}}\,]$ is formulated as a function of $z_{inv} = max(z^*_{inv}, z_{LCL})$ instead of z^*_{inv} (where z^*_{inv} is the inversion height directly obtained from Eq.(5) without any clipping, such that z^*_{inv} can be lower than z_{LCL}), this case of $z^*_{inv} < z_{LCL}$ is diagnosed as a highly cloudy condition in the current ELF. It seems that an advanced ELF needs to be able to simulate the decrease in LCA with the increase in the absolute value of $z^*_{DL} \equiv z^*_{inv} - z_{LCL}$, such as ELF=$f \cdot [\, 1 - (z_{LCL}/\Delta z_s)\sqrt{1 + a \cdot \delta^2_*}\,]$, where $\delta_* \equiv z^*_{DL}/z_{LCL}$ is a generalized decoupling parameter and a is a positive constant. This approach is likely to relocate the observation frequency of ~~CL0~~ noCL in the high ELF bins into the low ELF bins (Figs. ~~6i~~ 7i and j), reduce the large ELF values for ~~CL0~~ noCL (Figs. ~~5g~~ 6g and h), and improve the non-centered correlations between ΔELF and ΔLCA for various CL types including ~~CL0~~ noCL (Figs. ~~2 and~~ 3 and 4).

Another apparent problem of the current ELF is the decrease in ELF over the desert areas (e.g., Sahara, Australia, and Saudi-Arabia) when ~~CL12~~ Cu was reported (see Figs. ~~3c and 3c~~4c and 4o). In contrast to the ocean where the onset of ~~CL12~~ Cu is often associated with the decoupling of PBL and the decreases in overlying marine stratocumulus and LCA (e.g., Bretherton (1992), Park et al. (2004)), the onset of ~~CL12~~ Cu over the deserts without the background stratocumulus seems to directly increase LCA. In this case, ELF tries to mimic the observed increase in LCA by decreasing LCL (see Fig. ~~3o~~S2c) but the larger increases in z_{inv} and associated PBL decoupling seem to offset the impact of the reduced LCL, resulting in the decrease in ELF. Conceptually, current ELF is designed to mainly diagnose the variations in stratiform clouds and detrained cumulus at the inversion base, not the cumulus updraft plume itself (see Fig. 1 of PS19), which is reflected in part by the higher non-centered correlations between ΔELF and ΔAWP for stratiform clouds than for convective clouds as shown in Figs. ~~2 and 3.~~ 3 and 4. To further improve the performance of ELF, it seems to be necessary to additionally diagnose the fraction of cumulus updraft plume, particularly, in the regions without background stratiform clouds, such as deserts. Because the onset of ~~CL12~~ Cu is closely associated with the PBL decoupling, one plausible approach is to incorporate a process to increase ELF as δ_* increases, such that it can offset the decreases in stratocumulus and ELF with increasing δ_*. If the aforementioned ELF=$f \cdot [\, 1 - (z_{LCL}/\Delta z_s)\sqrt{1 + a \cdot \delta^2_*}\,]$ is adopted as an advanced ELF, the contribution of cumulus updraft plume can be incorporated by setting a to be smaller (or even negative) than the default case excluding the contribution of cumulus updraft plume. Potentially, a could be parameterized as a decreasing function of z_{LCL}.

Figures ~~8c-f~~ 9c-f show the variations in z_{LCL}, z_{inv}, $\sqrt{z_{LCL} \cdot z_{inv}}$, and α as a function of ELF and LCA when ~~CL5 and CL12~~ Sc and Cu were reported over the ocean and land, respectively. When averaged over the entire bins (the 'all' bin in the right most column in each plot), ~~CL12~~ Cu has higher z_{LCL}, z_{inv}, and α than ~~CL5~~Sc, which is consistent with our conceptual understanding. The increase in ~~CL12~~ Cu AWP from the zero to one-octa bins over land is accompanied by the rapid increase in α (black solid line in Fig. ~~8f~~9f), presumably reflecting the onset of cumulus updraft plume as the PBL is decoupled which, as mentioned before, is not correctly captured by current ELF (black dotted line in Fig. ~~8f~~9f). For both ~~CL5 and CL12~~ Sc and Cu (and also other CLs, not shown), z_{LCL} tends to decrease monotonically with LCA and ELF, however, z_{LCL} and z_{inv} decrease more rapidly with ELF than with LCA. As a result, the decreasing rate of $\sqrt{z_{inv} \cdot z_{LCL}}$ with ELF is much larger than that with AWP (green lines in Figs. ~~8c-f~~9c-f). One simple way to remedy this problem is to parameterize the scale

height Δz_s in ELF$= f \cdot (1 - \sqrt{z_{inv} \cdot z_{LCL}}/\Delta z_s)$ as a function of appropriate environmental variables, such as z_{inv}, z_{LCL}, and $q_{v,sfc}$. To check whether this is a possible approach, we computed an ideal scale height $\Delta z_{s,i}$ in an adhoc manner, such that it exactly reproduces the observed LCA. More specifically, for individual data points shown in Figs. ~~5g and 5h~~6g and 6h, we computed $\Delta z_{s,i} = (\sqrt{z_{inv} \cdot z_{LCL}})/(1 - AWP/f)$ by inverting Eq.(~~3~~4) (here, we implicitly assumed that Δz_s used in Eq.(~~3~~4) for deriving ELF differs from $\Delta z_s = 2750$ [m] used in Eq.(5) for deriving z_{inv}, which is a completely reasonable assumption because there is no physical reason for Δz_s in both equations to be identical). Figures ~~8g and 8h~~ 9g and 9h show the distribution of $\Delta z_{s,i}$ in the phase space of z_{LCL} and $\delta \equiv z_{DL}/z_{LCL}$ over the ocean and land, respectively. As shown, $\Delta z_{s,i}$ has a large inter-CL spread (and also relatively smaller seasonal and diurnal spreads) instead of being a constant 2750 [m]. There is a tendency for fog and stratus to have larger $\Delta z_{s,i}$ than ~~CL0~~ noCL and convective clouds and to the first order, $\Delta z_{s,i}$ seems to increase as δ increases and z_{LCL} decreases. Various CLs, each of which have their own distinct PBL structure and AWP, seem to be reasonably separated from each other in this phase diagram, implying a possibility to parameterize Δz_s as a function of z_{LCL} and δ. Because an advanced ELF needs to incorporate other aspects discussed in the above two paragraphs, which will presumably involve some changes in the functional form of ELF, we leave a detailed parameterization of Δz_s for future research.

4 Summary and Conclusion

We extended the previous work of Park and Shin (2019), to examine the relationship between various proxies (i.e., LTS, EIS, ECTEI, and ELF) and LCA of individual low-level cloud types (CL). An individual CL has its own distinct PBL structure, such that detailed analysis of the relationship between various proxies and LCA of individual CL can provide insights into the strength and weakness of individual proxies, which may help to develop a better proxy in future.

Firstly, we compared the annual climatology and seasonal cycle of individual CL's frequency (~~Fig~~Figs. 1 ~~). CL0~~ and 2). noCL is frequently reported over the winter continents and Arctic area but is seldom reported over the open ocean except in the eastern equatorial SST cold tongue region where PBL is stable in association with negative surface buoyancy flux. By construction, ELF has a limitation in correctly diagnosing reduced cloudiness with enhanced stability in this region. ~~CL11 and CL6~~ Fog and F.St are frequently observed over the summer western North Pacific/Atlantic oceans and Arctic area, presumably due in part to the cooling of northward advected air parcels and enhanced upward moisture flux through the ice-free Arctic ocean during summer. These processes can be captured by ELF through the decrease in z_{LCL}. Over the North Pacific and Atlantic oceans, ~~CL7 and CL39~~ B.St and Cb are more frequently observed during DJF in association with the frequent passage of synoptic storms and the formation of ~~CL7 (CL39~~B.St (Cb) on the front (rear) side of warm (cold) front where lower tropospheric stability is higher (smaller) than the climatology, which can be captured by ELF through the changes of z_{inv}. ~~CL5~~ Sc is frequently observed over the eastern subtropical and midlatitude oceans during JJA and inter-seasonal variations in ~~CL12 and CL39~~ Cu and Cb over most ocean areas tend to be opposite to those of ~~CL5~~Sc. ELF is designed to capture these conversions between stratocumulus and cumulus in association with the PBL decoupling.

We then examined the relationship between the anomalies of various proxies and AWP with respect to the climatology when a specific CL was reported in each grid box (Figs. ~~2 and~~ 3 and 4). When ~~CL0~~ noCL was reported, LTS/EIS does not capture the decrease in LCA and ELF has a similar problem except over the northern continents during winter where the freezedry factor operates. When stratiform clouds are reported, ELF captures the increase in LCA very well due to the simultaneous decreases in z_{LCL}, z_{inv}, and α. With the exception of over the far northern continent and Arctic area, LTS/EIS works well also, but their performance for ~~CL6 and CL7~~ F.St and B.St are degraded mainly due to undesirable anomalies over the Asia and Arctic area. As well as fog and stratus, ELF captures the variations in LCA when stratocumulus and cumulus are reported reasonably well and significantly better than LTS and EIS. However, when ~~CL12~~ Cu was reported over Asia and most desert areas, ELF, as well as LTS/EIS, had a problem in capturing the increase in LCA. ELF shows more consistent inter-CL variations with the AWP of individual CL than LTS and EIS, which have too strong ocean-land contrasts and seasonal cycle over land (Fig. ~~4~~5). The scatter plots between various proxies and individual CL's AWP showed that if ~~CL0~~ noCL is excluded, all LTS/EIS/ELF have very good correlations with the AWP of individual CLs, although ELF perform slightly better than LTS and EIS (Fig. ~~5~~6). To be a better proxy for LCA, the ELF for ~~CL0 and CL12~~ noCL and Cu over ocean and nocturnal land should be reduced, while the ELF for ~~CL11 and CL12~~ Fog and Cu over land during the day time should be enhanced.

We also analyzed individual CL's frequency in the bins of various proxies. In the case of the perfect proxy for LCA (i.e., LCA itself), the frequency of ~~CL12~~ Cu (stratiform clouds) decreases (increases) with LCA; convective clouds are mostly observed during the day, particularly over land; ~~CL0~~ noCL exists entirely in the zero octa bin; the bin AWP increases in a perfect linear way as LCA increases; and the observation number FQ is the largest in the zero (particularly, over land) and 8 octa bins. Similar to the perfect proxy, all LTS/EIS/ELF simulate the decrease in ~~CL12 FQ (~~Cu FQ (increase in stratiform clouds FQ) from the low to high bins reasonably. However, all proxies incorrectly diagnose the observed no low-level cloud conditions (~~CL0~~noCL) as cloudy conditions (more severely for LTS/EIS), resulting in unrealistic distributions of the bin AWP and observation number FQ across the bins. The analysis of spatial-seasonal correlation reveals that LCA increases as the frequencies of sky-obscuring fog, stratus, stratocumulus, and continental convective clouds increase, and decreases as the frequencies of ~~CL0~~ noCL and marine convective clouds increase. Except for marine ~~CL84 and continental CL12~~Sc-Cu and continental Cu, ELF reproduces these observed characteristics much better than LTS/EIS, which, in particular, suffers from an unrealistically strong positive spatial-seasonal correlation with the ~~CL0~~ noCL frequency. Similar to the aforementioned analysis of CL's frequencies, all LTS/EIS/ELF do not correctly reproduce the observed monotonic increase in the bin cloud AMT, due mainly to the incorrect diagnosis of ~~CL0~~ noCL as cloudy conditions, although ELF performs better than LTS/EIS. The analysis of spatial-seasonal correlations between the AMT of individual CL and various proxies indicates that a superior performance of ELF to LTS/EIS as a global proxy for LCA comes from its realistic correlations with various CLs rather than with a specific CL.

Finally, to provide a potential pathway for an advanced ELF in future, we examined in more detail the cases when ELF performs poorly. When ~~CL0~~ noCL is reported and so LCA decreases, ELF increases undesirably from its climatological value at each grid point, which is speculated to be associated with the constraint that forces z_{inv} to be larger than z_{LCL}. Because low-level cloud cannot be formed when the inversion height is lower than z_{LCL}, current ELF is likely to mis-diagnose ~~CL0~~ noCL as cloudy conditions. It is necessary to allow $z_{DL} = z_{inv} - z_{LCL}$ to be negative and reformulate ELF to appropriate

handle the negative z_{DL}. When ~~CL12~~ Cu is reported over the deserts where background stratiform clouds do not exist, LCA increases but ELF decreases undesirably from its climatological value. This is presumably because current ELF is designed to handle the variations in stratiform clouds and detrained cumulus at the inversion base, not the cumulus updraft plume itself. An advanced ELF needs to diagnose the fraction of cumulus updraft plume, also. Current ELF=$f \cdot (1 - \sqrt{z_{inv} \cdot z_{LCL}}/\Delta z_s)$ assumes a constant scale height, Δz_s=2750 [m]; however, it turns out that the ideal Δz_s allowing ELF to exactly diagnose the observed AWP of individual CLs has a large inter-CL spread, implying a need to parameterize Δz_s as a function of appropriate variables~~, if any~~. One possible way of addressing these problems is to formulate ELF=$f \cdot [\ 1 - (z_{LCL}/\Delta z_s)\sqrt{1 + a \cdot \delta_*^2}\ ]$, where $\delta_* \equiv (z_{inv}^* - z_{LCL})/z_{LCL}$ and z_{inv}^* is allowed to be lower than z_{LCL}, and then parameterize a and Δz_s as a function of appropriate environmental variables. The formulation of an advanced ELF is more complicated than LTS/EIS/ECTEI and could be somewhat empirical (however, we note that the environmental variables used for ELF are identical to the ones used for ECTEI). Given the fact that ELF has performed as a good global proxy for LCA in various cloud regimes, it may be worthwhile to develop an advanced ELF. Although not shown here, we checked that the observed significant correlations between ELF and LCA were also simulated by the Community Atmosphere Model version 5 (CAM5, Park et al. (2014)) and the Seoul National University Atmosphere Model version 0 with a Unified Convection Scheme [SAM0-UNICON, Park et al. (2019, 2017), Park (2014a, b)]~~, which, in~~ . We are planning to compare cloud feedback estimated by ELF with those estimated by LTS/EIS/ECTEI and observations. In addition to the derivation of an advanced ELF ~~,~~and aforementioned analysis of various GCM simulations, the analysis of cloud feedback and associated climate sensitivity will be reported in the near future.

Data availability. The EECRA cloud data used in our study is available at https://rda.ucar.edu/datasets/ds292.2/. The ERA-interim reanalysis data used in our study is available at https://rda.ucar.edu/datasets/ds627.0/.

Author contributions. Sungsu Park guided the research and Jihoon Shin conducted the overall analysis under the supervision of Sungsu Park.

Competing interests. The authors declare that they have no conflict of interest.

Acknowledgements. ~~This work was supported by the Creative-Pioneering Researchers Program of~~ The authors are supported by Seoul National University (SNU~~; 3345-20180018~~).

References

Albrecht, B. A., Betts, A. K., Schubert, W. H., and Cox, S. K.: Model of the thermodynamic structure of the trade-wind boundary layer: Part I. Theoretical formulation and sensitivity tests, Journal of the Atmospheric Sciences, 36, 73–89, 1979.

Andrews, T., Gregory, J. M., Webb, M. J., and Taylor, K. E.: Forcing, feedbacks and climate sensitivity in CMIP5 coupled atmosphere-ocean climate models, Geophysical Research Letters, 39, 2012.

Augstein, E., Schmidt, H., and Ostapoff, F.: The vertical structure of the atmospheric planetary boundary layer in undisturbed trade winds over the Atlantic Ocean, Boundary-Layer Meteorology, 6, 129–150, 1974.

Betts, A. K. and Ridgway, W.: Coupling of the radiative, convective, and surface fluxes over the equatorial Pacific, Journal of the atmospheric sciences, 45, 522–536, 1988.

Bony, S. and Dufresne, J.-L.: Marine boundary layer clouds at the heart of tropical cloud feedback uncertainties in climate models, Geophysical Research Letters, 32, 2005.

Bretherton, C.: A conceptual model of the stratocumulus-trade-cumulus transition in the subtropical oceans, in: Proc. 11th Int. Conf. on Clouds and Precipitation, vol. 1, pp. 374–377, International Commission on Clouds and Precipitation and International Association of Meteorology and Atmospheric Physics Montreal, Quebec, Canada, 1992.

Brient, F. and Bony, S.: How may low-cloud radiative properties simulated in the current climate influence low-cloud feedbacks under global warming?, Geophysical Research Letters, 39, 2012.

Caldwell, P. M., Zhang, Y., and Klein, S. A.: CMIP3 subtropical stratocumulus cloud feedback interpreted through a mixed-layer model, Journal of Climate, 26, 1607–1625, 2013.

Cess, R. D., Potter, G., Blanchet, J., Boer, G., Del Genio, A., Deque, M., Dymnikov, V., Galin, V., Gates, W., Ghan, S., et al.: Intercomparison and interpretation of climate feedback processes in 19 atmospheric general circulation models, Journal of Geophysical Research: Atmospheres, 95, 16 601–16 615, 1990.

Collins, W. D., Rasch, P. J., Boville, B. A., Hack, J. J., McCaa, J. R., Williamson, D. L., Kiehl, J. T., Briegleb, B., Bitz, C., Lin, S., et al.: Description of the NCAR community atmosphere model (CAM 3.0), NCAR Tech. Note NCAR/TN-464+ STR, 226, 2004.

Deser, C. and Wallace, J. M.: Large-scale atmospheric circulation features of warm and cold episodes in the tropical Pacific, Journal of Climate, 3, 1254–1281, 1990.

Hahn, C. J. and Warren, S. G.: Extended edited synoptic cloud reports from ships and land stations over the globe, 1952-1996, Environmental Sciences Division, Office of Biological and Environmental Research, US Department of Energy, 1999.

Kawai, H., Koshiro, T., and Webb, M. J.: Interpretation of Factors Controlling Low Cloud Cover and Low Cloud Feedback Using a Unified Predictive Index, Journal of Climate, 30, 9119–9131, 2017.

Klein, S. A. and Hartmann, D. L.: The seasonal cycle of low stratiform clouds, Journal of Climate, 6, 1587–1606, 1993.

Koshiro, T. and Shiotani, M.: Relationship between low stratiform cloud amount and estimated inversion strength in the lower troposphere over the global ocean in terms of cloud types, Journal of the Meteorological Society of Japan. Ser. II, 92, 107–120, 2014.

Mansbach, D. K. and Norris, J. R.: Low-level cloud variability over the equatorial cold tongue in observations and models, Journal of climate, 20, 1555–1570, 2007.

Nam, C., Bony, S., Dufresne, J.-L., and Chepfer, H.: The 'too few, too bright'tropical low-cloud problem in CMIP5 models, Geophysical Research Letters, 39, 2012.

Norris, J. R.: Low cloud type over the ocean from surface observations. Part II: Geographical and seasonal variations, Journal of climate, 11, 383–403, 1998.

Norris, J. R. and Klein, S. A.: Low cloud type over the ocean from surface observations. Part III: Relationship to vertical motion and the regional surface synoptic environment, Journal of climate, 13, 245–256, 2000.

Park, S.: A unified convection scheme (UNICON). Part I: Formulation, Journal of the Atmospheric Sciences, 71, 3902–3930, 2014a.

Park, S.: A unified convection scheme (UNICON). Part II: Simulation, Journal of the Atmospheric Sciences, 71, 3931–3973, 2014b.

Park, S. and Leovy, C. B.: Marine low-cloud anomalies associated with ENSO, Journal of Climate, 17, 3448–3469, 2004.

Park, S. and Shin, J.: Heuristic estimation of low-level cloud fraction over the globe based on a decoupling parameterization, Atmospheric Chemistry and Physics, 19, 5635–5660, 2019.

Park, S. and Shin, J.: Relationship between Low-level Clouds and Large-scale Environmental Conditions around the Globe, In Preparation, 2020.

Park, S., Leovy, C. B., and Rozendaal, M. A.: A new heuristic Lagrangian marine boundary layer cloud model, Journal of the atmospheric sciences, 61, 3002–3024, 2004.

Park, S., Bretherton, C. S., and Rasch, P. J.: Integrating cloud processes in the Community Atmosphere Model, version 5, Journal of Climate, 27, 6821–6856, 2014.

Park, S., Baek, E.-H., Kim, B.-M., and Kim, S.-J.: Impact of detrained cumulus on climate simulated by the Community Atmosphere Model Version 5 with a unified convection scheme, Journal of Advances in Modeling Earth Systems, 3, 2017.

Park, S., Shin, J., Kim, S., Oh, E., and Kim, Y.: Global climate simulated by the seoul national university atmosphere model version 0 with a unified convection scheme (sam0-unicon), Journal of Climate, 2019.

Qu, X., Hall, A., Klein, S. A., and Caldwell, P. M.: On the spread of changes in marine low cloud cover in climate model simulations of the 21st century, Climate dynamics, 42, 2603–2626, 2014.

Qu, X., Hall, A., Klein, S. A., and Caldwell, P. M.: The strength of the tropical inversion and its response to climate change in 18 CMIP5 models, Climate Dynamics, 45, 375–396, 2015.

Simmons, A., Uppala, S., Dee, D., and Kobayashi, S.: ERA-Interim: New ECMWF reanalysis products from 1989 onwards, ECMWF newsletter, 110, 25–35, 2007.

Slingo, J.: The development and verification of a cloud prediction scheme for the ECMWF model, Quarterly Journal of the Royal Meteorological Society, 113, 899–927, 1987.

Stephens, G. L.: Cloud feedbacks in the climate system: A critical review, Journal of climate, 18, 237–273, 2005.

Vavrus, S. and Waliser, D.: An improved parameterization for simulating Arctic cloud amount in the CCSM3 climate model, Journal of Climate, 21, 5673–5687, 2008.

WMO: Manual on the observation of clouds and other meteors: Volume I, WMO Publication 407, 1975a.

WMO: Manual on the observation of clouds and other meteors, WMO Publication, 1, 1–155, 1975b.

Wood, R.: Stratocumulus clouds, Monthly Weather Review, 140, 2373–2423, 2012.

Wood, R. and Bretherton, C. S.: On the relationship between stratiform low cloud cover and lower-tropospheric stability, Journal of climate, 19, 6425–6432, 2006.

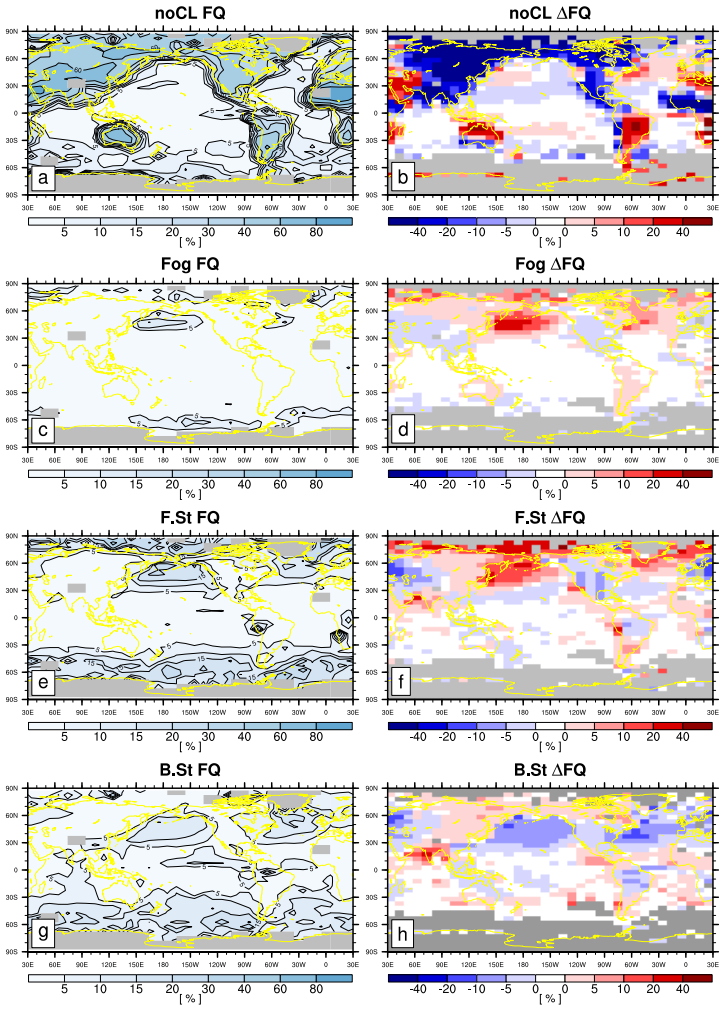

Figure 1. (First column) The annual mean climatological CL frequency (FQ) and (second column) the differences of climatological CL FQ between JJA and DJF [ΔFQ = FQ(JJA) - FQ(DJF)] for (a)~~CL0,~~ (b) ~~CL1~~noCL, (c)~~CL6,~~ (d) ~~CL7~~Fog, (e)~~CL5,~~ (f) ~~CL84,~~ F.St, and (g)~~CL12, and~~ (h) B.St. In the first column, the grid boxes with total observation number less than 100 are ~~marked with a dot~~shaded with a gray color. In the second column, statistically insignificant ΔFQ at the 99.9 % confidence level from the two-sided Student t-test assuming independent samples are denoted by white color~~. Grid~~ , and the grid boxes with the observation number less than 100 during either JJA or DJF are shaded with a gray color.

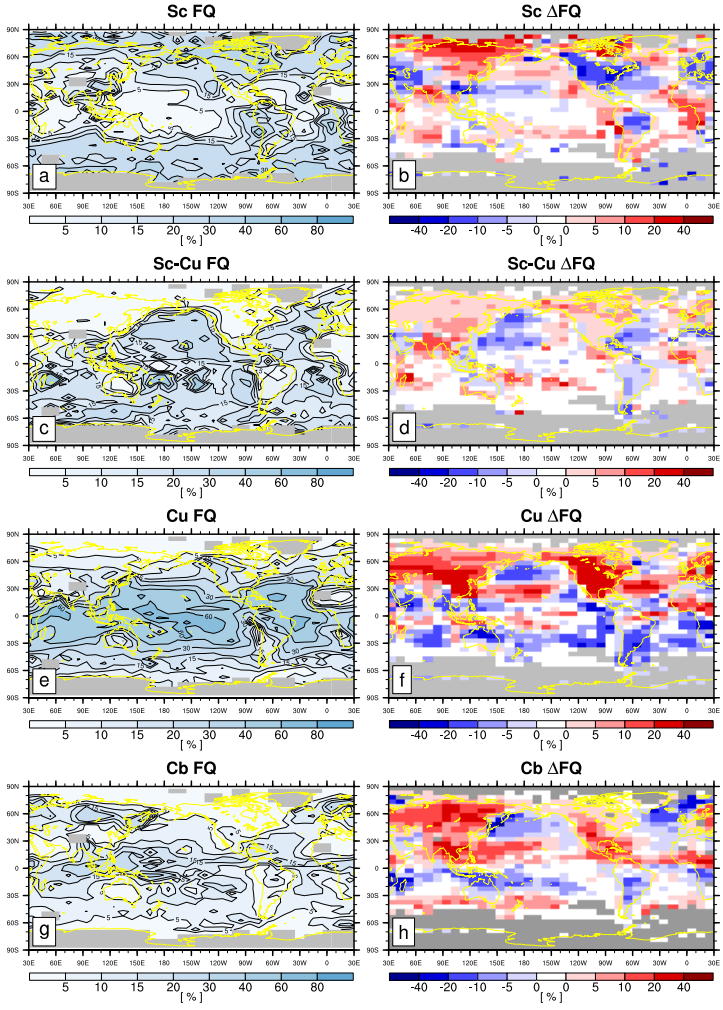

Figure 2. Same as Fig. 1 but for Sc, Sc-Cu, Cu, and Cb.

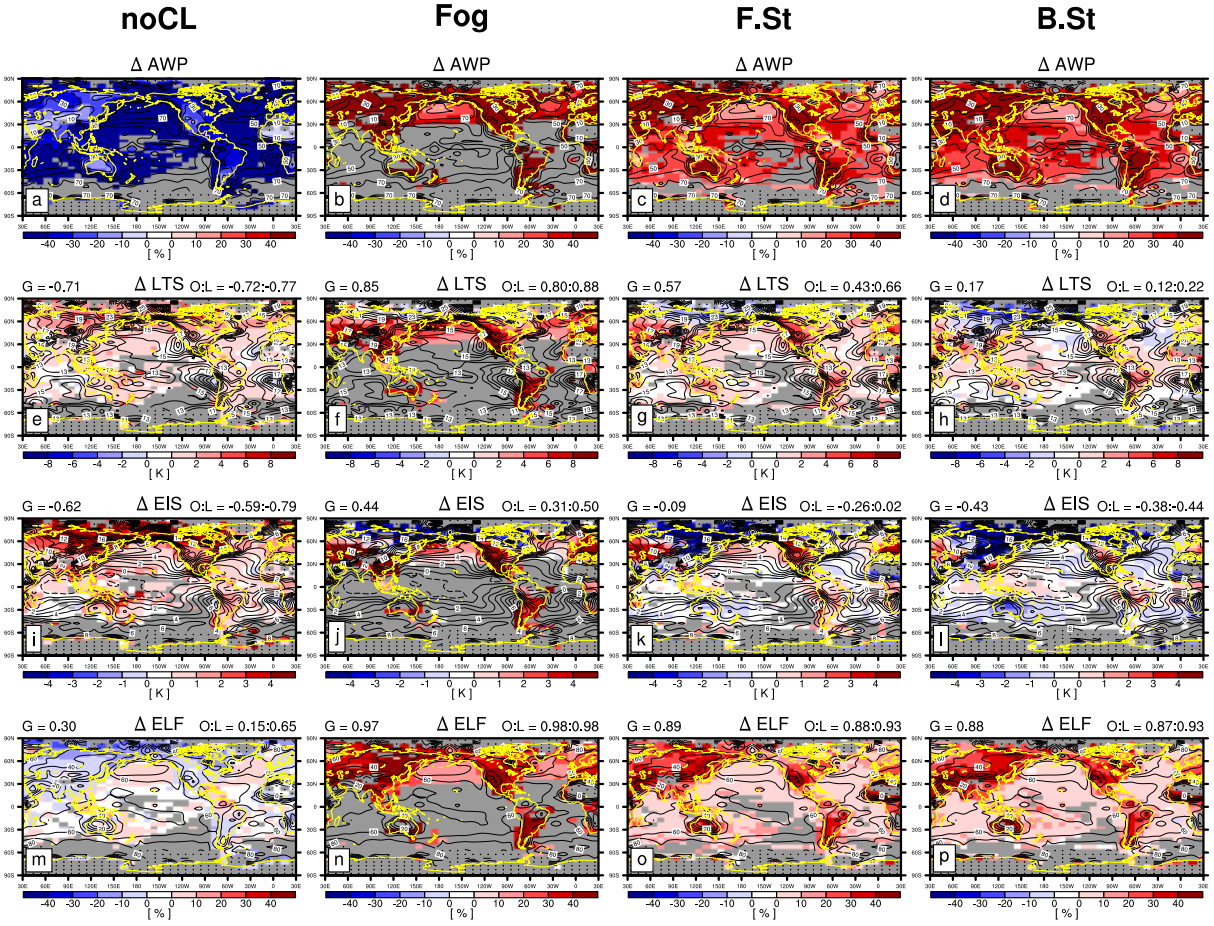

Figure 3. Composite anomalies of (1st row) AWP (amount-when-present), (2nd) LTS, (3rd) EIS, and (4th) ~~z_{LCL}, (5th) z_{inv}, (6th) α, (7th) $1 - \beta_2$, and (8th)~~ ELF with respect to the annual climatology when (first column) ~~CL0~~noCL, (2nd) ~~CL1~~Fog, (3rd) ~~CL6~~F.St, and (4th) ~~CL7~~ B.St was reported. ΔAWP is the difference between the AWP of a specific CL and climatological LCA. Contour line is the annual climatology of LCA and individual proxies. At the top of individual plot, non-centered correlation coefficients between ΔAWP and Δproxy over the globe (G), ocean (O) and land (L) are shown. ~~Grid~~ In each plot, statistically insignificant anomalies at the 99.9 % confidence level from the two-sided Student t-test assuming independent samples are denoted by white color, and grid boxes with the observation number of a specific CL less than 100 are shaded by gray color. ~~The other conventions are the same as those of Fig. 1.~~ Grid boxes with total observation number less than 100 are marked with a dot.

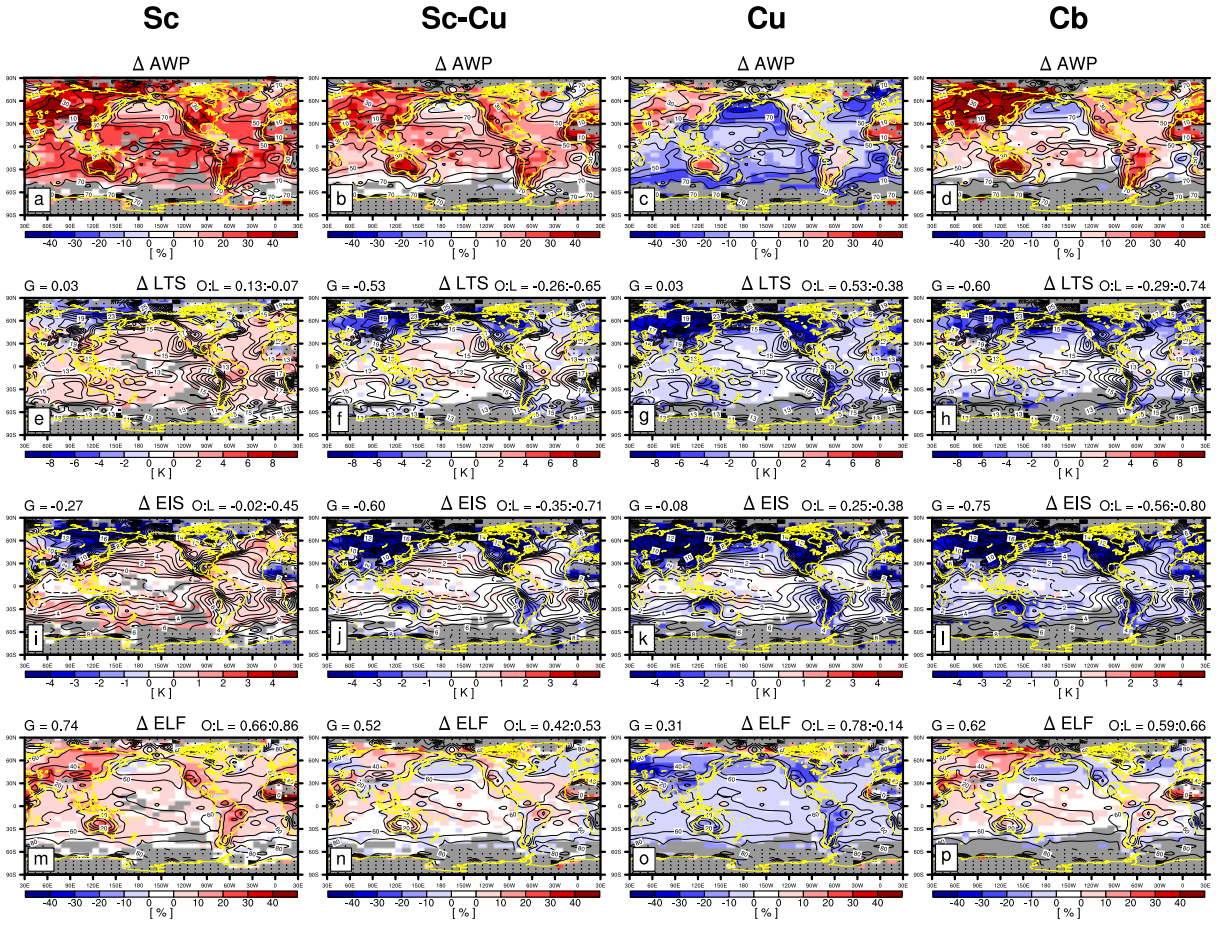

Figure 4. Same as Fig. ~~2 but for CL5, CL84, CL12, and CL39~~3 but for Sc, Sc-Cu, Cu, and Cb.

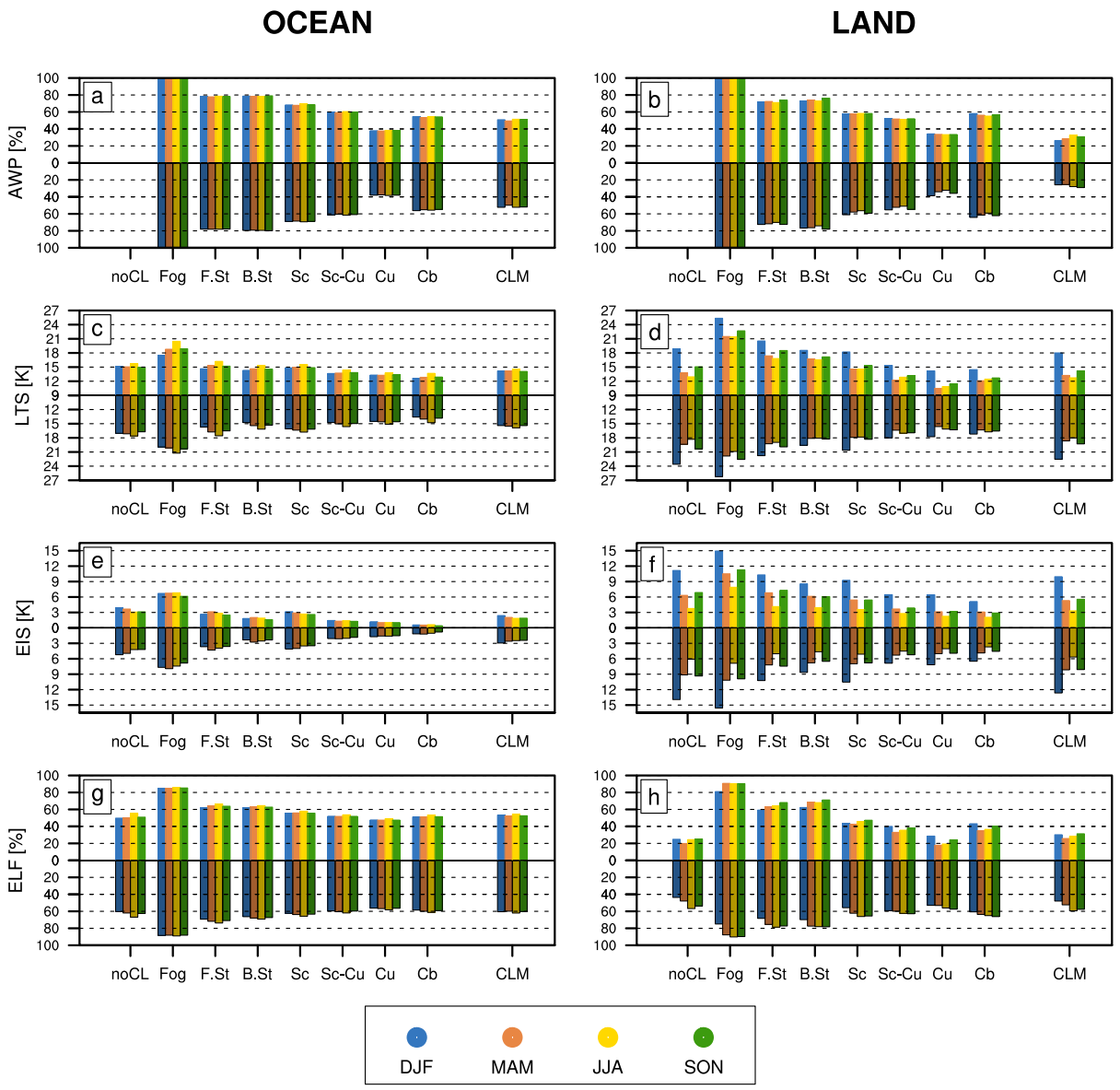

Figure 5. Seasonal climatologies of the (~~top~~ 1st row) AWP~~and (the other rows) various proxies~~ , (2nd) LTS, (3rd) EIS, and (4th) ELF averaged over the (left) ocean and (right) land for each season (DJF, MAM, JJA, SON denoted by different colors) during the daytime (09 am - 09 pm, upward bars with bright colors) and nighttime (09 pm - 09 am, downward bars with dark colors), respectively, when a specific CL was reported. In each plot, CLM denotes the climatology for all CLs.

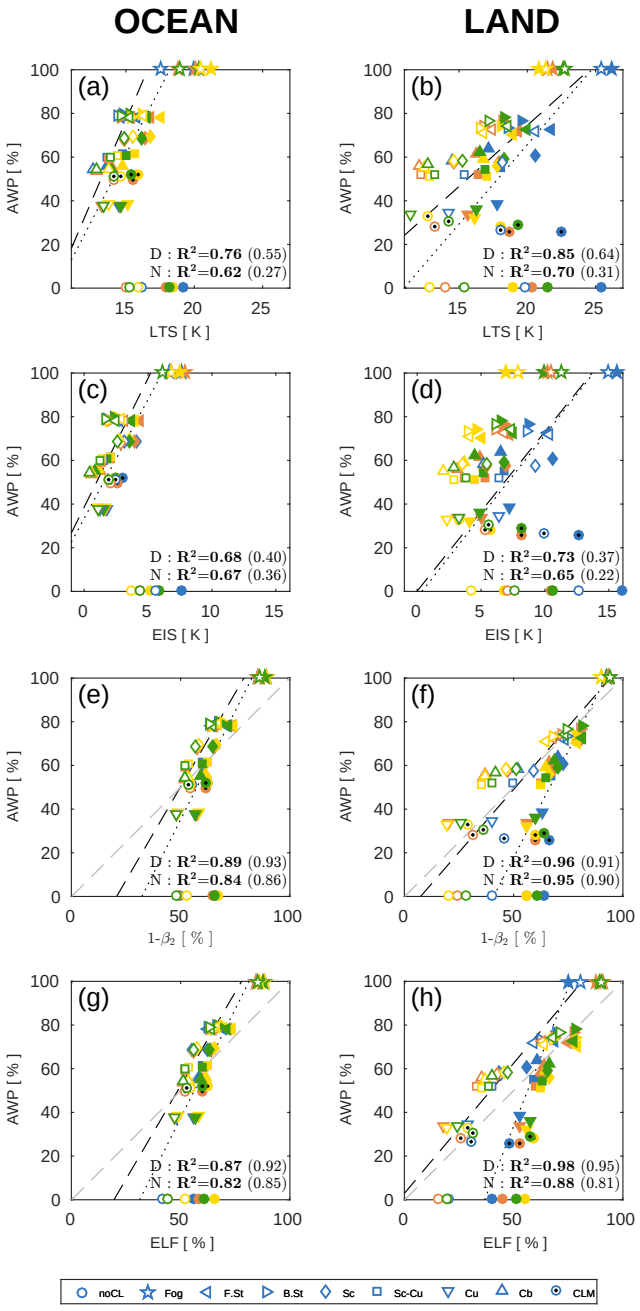

Figure 6. Scatter plots of Fig. ~~4~~ 5 over the (left) ocean and (right) land during the daytime (open symbols) and nighttime (filled symbols), respectively. Also plotted are the linear regression lines and squared correlation coefficients (R^2) during the daytime (D, dashed) and nighttime (N, dotted), respectively. The bold R^2 are the values when CLM and noCL are excluded in the regression analysis, and the R^2 in the parenthesis are the values when Fog is additionally excluded. The seasons were marked with the same colors as Fig. 5. The dashed gray lines in the last four plots denote AWP=ELF. ~~The CLM and CL0 cases are not included in the regression analysis.~~

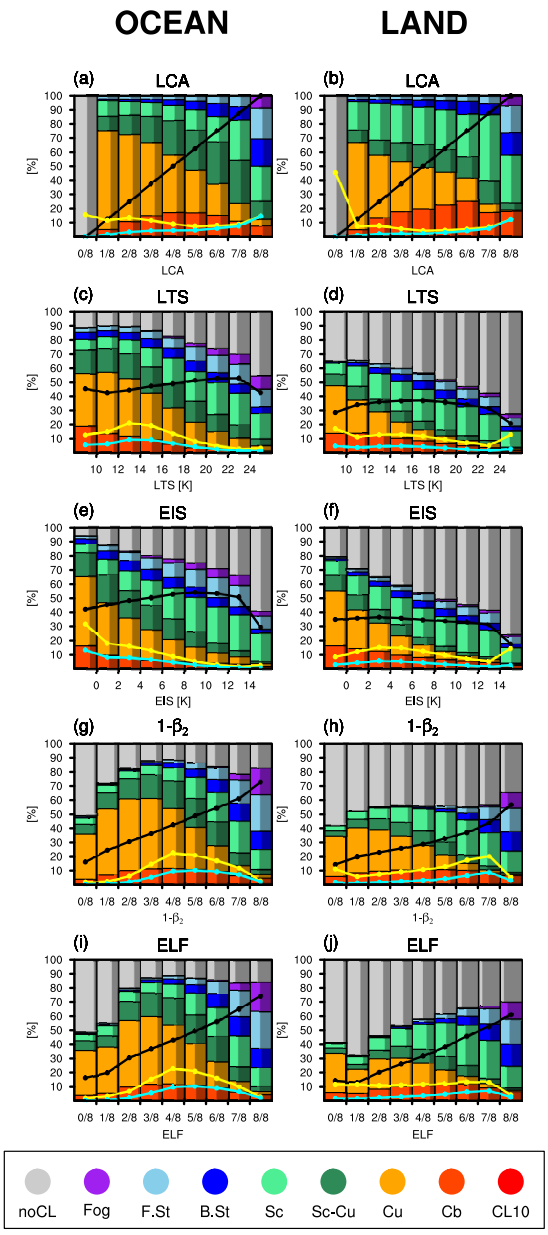

Figure 7. ~~Cumulative FQ~~ Stacked percentage plots for the FQs of individual CLs in the bins of various proxies, (a),(b) LCA (i.e., a perfect proxy for LCA), (c),(d) LTS, (e),(f) EIS, (g),(h) 1-β_2, and (i),(j) ELF over the (left) ocean and (right) land, respectively. AWP of all CLs in each bin is denoted by the black line. The observation number FQ of individual bin (the ratio of the observation number in each bin to the total observation number of entire bins) is denoted by the yellow line. LCA in each bin is denoted by the cyan line, which is the product of the black and yellow lines. The sum of the yellow line integrated over the entire bins is ~~100.~~ 100%. The sum of the cyan line integrated over the entire bins is the global-annual mean LCA. The bright and dark colors in each bar denote the fractions during the daytime and nighttime, respectively.

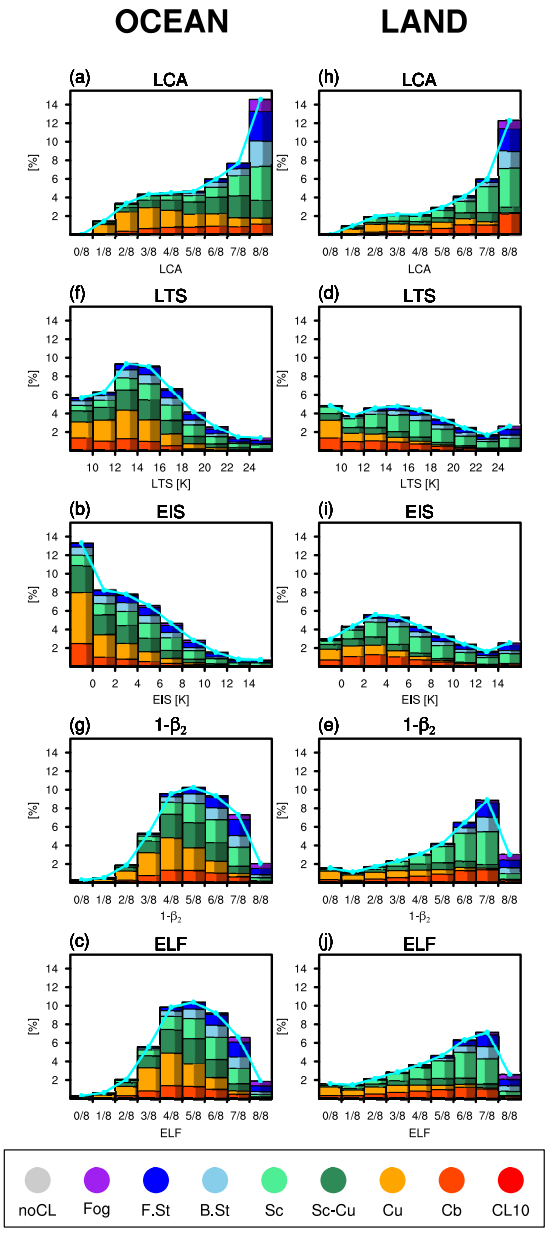

Figure 8. Same as Fig. ~~6 but for cumulative~~ 7 but for AMT of individual CL in each bin. The cyan lines are identical to those shown in Fig. ~~6.~~ 7. The sum of all CLs' AMT integrated over the entire bins is the global annual-mean LCA, which is identical regardless of the proxies used for the composite.

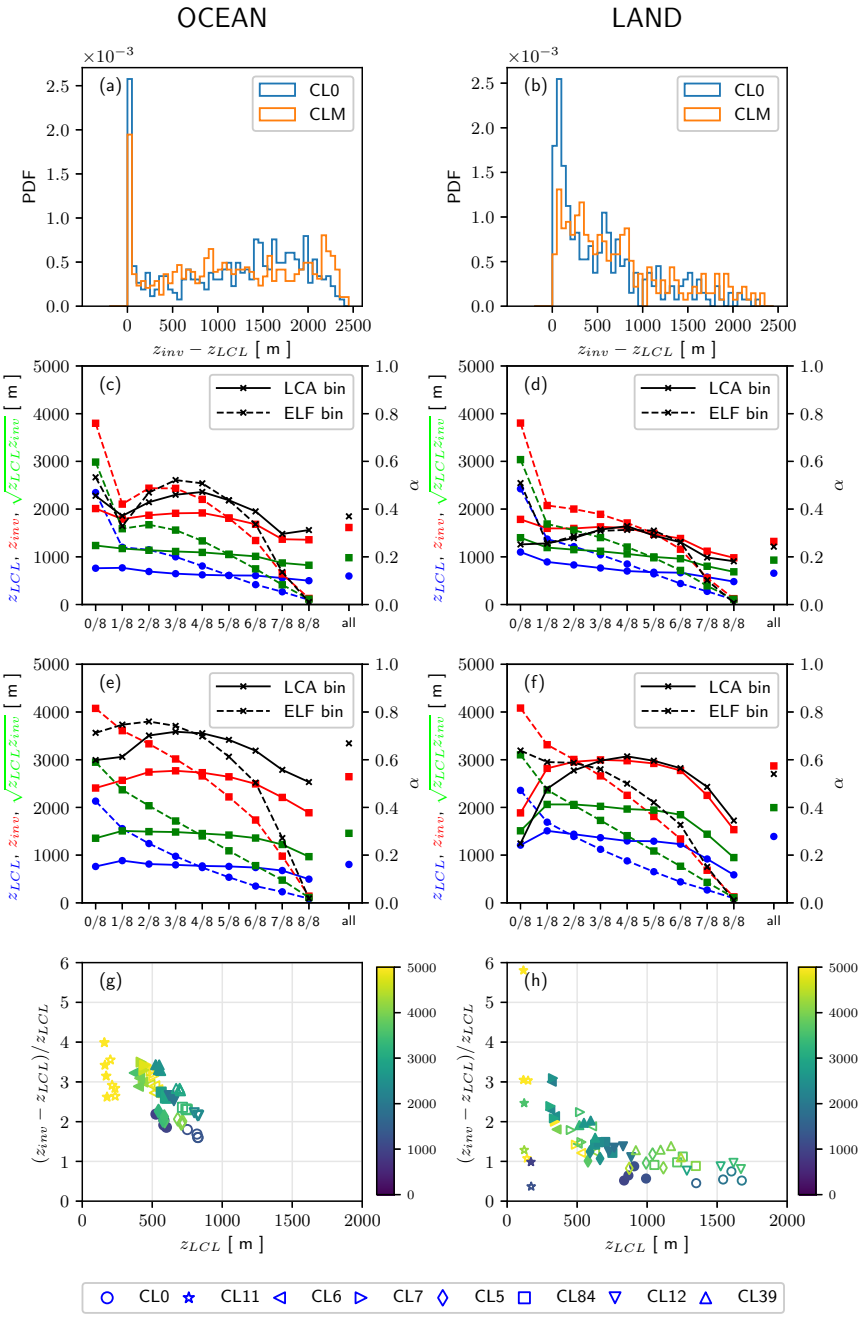

Figure 9. (a),(b) Probability density functions (PDF) of $z_{DL} = z_{inv} - z_{LCL}$ when ~~CL0~~ noCL was reported (blue) and any CL was reported (red); (c)-(f) z_{LCL} (blue), z_{inv} (red), α (black), and $\sqrt{z_{LCL} \cdot z_{inv}}$ (green) in each octa bins of LCA (solid lines) and ELF (dashed lines) when [(c),(d)] ~~CL5~~ Sc was reported and (e),(f) ~~CL12~~ Cu was reported, with the values averaged over the entire bins denoted by 'all' in the right most column; and [(g),(h)] the distribution of $\Delta z_{s,i} = (\sqrt{z_{inv} \cdot z_{LCL}})/(1 - AWP/f)$ (shaded; in units of meter) as a function of z_{LCL} and $\delta \equiv z_{DL}/z_{LCL}$ for individual data points shown in Figs. ~~5g and 5h~~6g and 6h. The plots on the left and right columns are over the ocean and land, respectively.

Table 1. Low-level cloud (CL) specified by WMO (CL0-CL9). EECRA defined two additional CLs - CL10 and CL11. When multiple CLs exist, the observer is allowed to report only one CL as a representative CL following the coding priority. Among four cloud types (CL1, CL5, CL6, and CL7), the cloud type that has the largest sky fraction has the highest priority. 'Bad weather' denotes the conditions that generally exist during precipitation and a short time before and after.

CL code	Nontechnical Description	Coding Priority	Short Name
0	No stratocumulus, stratus, cumulus, or cumulonimbus	10	No Low-Cloud
1	Cumulus with little vertical extent and seemingly flattened or ragged cumulus other than of bad weather, or both.	By Cover	Shallow Cumulus
2	Cumulus of moderate or strong vertical extent, generally with protuberances in the form of domes or towers, either accompanied or not by other cumulus or by stratocumulus,	5	Moderate Cumulus
3	Cumulonimbus, the summits of which at least partially lack sharp outlines but are neither clearly fibrous (cirriform) nor in the form of an anvil; cumulus, stratocumulus, or stratus may also be present	2	Cumulonimbus
4	Stratocumulus formed by the spreading out of cumulus; cumulus may also be present	3	Stratocumulus from Cumulus
5	Stratocumulus not resulting from the spreading out of cumulus	By Cover	Stratocumulus
6	Stratus in a more or less continuous sheet or layer, or in ragged shreds, or both, but no stratus fractus of bad weather	By Cover	Fair Weather Stratus
7	Stratus fractus of bad weather or cumulus fractus of bad weather, or both (pannus), usually below altostratus or nimbostratus	By Cover	Bad Weather Fractus
8	Cumulus and stratocumulus other than that formed from the spreading out of cumulus; the base of the cumulus is at a different level from that of the stratocumulus	4	Cumulus under Stratocumulus
9	Cumulonimbus, the upper part of which is clearly fibrous (cirriform) often in the form of an anvil, either accompanied or not by cumulonimbus without anvil or fibrous upper part, by cumulus, stratocumulus, stratus, or pannus	1	Cumulonimbus with Anvil
10	Sky is obscured (CL=missing with total cloud fraction N=9) by thunderstorm shower (ww=80-99)	·	Sky-obscuring TS (Thunderstorm Shower)
11	Sky is obscured (CL=missing with total cloud fraction N=9) by fog (ww=10-12, 40-49)	·	Sky-obscuring Fog

Table 2. Author-defined short names of low-level cloud (CL) types used in our study.

Abbreviation	CL code	Description
noCL	CL0	No Low-Level Cloud
Fog	CL11	Sky-Obscuring Fog
F.St	CL6	Fair Weather Stratus
B.St	CL7	Bad Weather Stratus
Sc	CL5	Stratocumulus
Sc-Cu	CL8 and CL4	Stratocumulus and Cumulus
Cu	CL1 and CL2	Cumulus
Cb	CL3 and CL9	Cumulonimbus

Table 3. Spatial-seasonal correlation coefficients between various proxies and the frequency (FQ) of individual CL. In contrast to Figs. ~~2 and~~ 3 and 4 where non-centered correlation coefficients were computed, the values in this table are the conventional centered-correlation coefficients computed from the climatological seasonal proxies obtained by using all observations in each seasonal grid box instead of the observations reporting a specific CL. In this table, LCA is a perfect proxy for LCA. Statistically significant correlations at the 99.9 % confidence level from the Student t test assuming independent samples are denoted by the bold characters.

CL	Domain	**LTS**	**EIS**	**$1-\beta_2$**	**ELF**	**LCA**
noCL	O	**0.69**	**0.79**	**0.42**	**-0.46**	**-0.62**
	L	**0.28**	**0.47**	**-0.33**	**-0.69**	**-0.87**
	G	**0.46**	**0.64**	**-0.19**	**-0.67**	**-0.82**
Fog	O	**0.45**	**0.23**	**0.55**	**0.63**	**0.49**
	L	**0.22**	**0.15**	**0.41**	**0.41**	**0.37**
	G	**0.20**	**0.07**	**0.47**	**0.55**	**0.53**
F.St	O	**0.32**	**0.52**	**0.75**	**0.70**	**0.56**
	L	**0.27**	**0.14**	**0.46**	**0.47**	**0.45**
	G	**0.22**	**0.27**	**0.61**	**0.60**	**0.54**
B.St	O	**-0.15**	**0.15**	**0.36**	**0.47**	**0.70**
	L	0.01	-0.00	**0.43**	**0.52**	**0.56**
	G	**-0.16**	**-0.06**	**0.38**	**0.52**	**0.69**
Sc	O	**0.40**	**0.59**	**0.66**	**0.39**	**0.31**
	L	**0.17**	**0.15**	**0.57**	**0.54**	**0.68**
	G	**0.30**	**0.40**	**0.56**	**0.36**	**0.31**
Sc-Cu	O	0.01	**-0.12**	**-0.08**	0.03	**0.28**
	L	**-0.29**	**-0.50**	**-0.07**	**0.18**	**0.33**
	G	**-0.22**	**-0.43**	**0.05**	**0.27**	**0.50**
Cu	O	**-0.36**	**-0.79**	**-0.78**	**-0.67**	**-0.53**
	L	**-0.49**	**-0.68**	**-0.30**	0.01	**0.19**
	G	**-0.45**	**-0.75**	**-0.30**	**-0.03**	**0.10**
Cb	O	**-0.46**	**-0.38**	**-0.20**	**-0.21**	**-0.08**
	L	**-0.17**	**-0.17**	**0.14**	**0.21**	**0.35**
	G	**-0.32**	**-0.31**	**0.03**	**0.08**	**0.17**
CLM	O	-	-	-	-	-
	L	-	-	-	-	-
	G	-	-	-	-	-

~~Same as Table 2 but for the amount (AMT) of individual CL.~~

Table 4. Same as Table 3 but for the amount (AMT) of individual CL.

CL	Domain	LTS	EIS	$1-\beta_2$	ELF	LCA
noCL	O	-	-	-	-	-
	L	-	-	-	-	-
	G	-	-	-	-	-
Fog	O	**0.45**	**0.23**	**0.55**	**0.63**	**0.49**
	L	**0.22**	**0.15**	**0.41**	**0.41**	**0.37**
	G	**0.20**	**0.07**	**0.47**	**0.55**	**0.53**
F.St	O	**0.32**	**0.51**	**0.76**	**0.72**	**0.60**
	L	**0.29**	**0.18**	**0.48**	**0.49**	**0.48**
	G	**0.22**	**0.27**	**0.62**	**0.62**	**0.58**
B.St	O	**-0.14**	**0.17**	**0.39**	**0.49**	**0.73**
	L	0.02	0.02	**0.44**	**0.52**	**0.57**
	G	**-0.14**	**-0.03**	**0.40**	**0.53**	**0.71**
Sc	O	**0.43**	**0.58**	**0.70**	**0.47**	**0.45**
	L	**0.23**	**0.19**	**0.61**	**0.58**	**0.72**
	G	**0.33**	**0.39**	**0.62**	**0.46**	**0.46**
Sc-Cu	O	**0.09**	-0.00	**0.07**	**0.18**	**0.47**
	L	**-0.24**	**-0.46**	0.00	**0.24**	**0.41**
	G	**-0.17**	**-0.37**	**0.14**	**0.35**	**0.61**
Cu	O	**-0.34**	**-0.74**	**-0.70**	**-0.59**	**-0.36**
	L	**-0.44**	**-0.63**	**-0.21**	**0.07**	**0.28**
	G	**-0.43**	**-0.73**	**-0.23**	**0.03**	**0.22**
Cb	O	**-0.37**	**-0.16**	-0.00	**-0.06**	**0.08**
	L	**-0.08**	**-0.04**	**0.26**	**0.28**	**0.40**
	G	**-0.22**	**-0.13**	**0.17**	**0.15**	**0.23**
CLM	O	**-0.20**	0.01	**0.48**	**0.81**	**1.00**
	L	**-0.06**	**-0.21**	**0.58**	**0.82**	**1.00**
	G	**-0.23**	**-0.23**	**0.54**	**0.84**	**1.00**